Search for solar chameleons and relic axions with CAST

June 8th, 2015

To be presented by:

G. Cantatore, L. Miceli and K. Zioutas,

on behalf of the CAST collaboration and the external collaborators

S. Baum and A. Upadhye

CERN-SPSC-2015-021 / SPSC-P-352
08/06/2015

1. **Introduction** – (responsible K. Zioutas)

In its first 15 years of existence, CAST equipment has been continuously upgraded. For example, the recycled X-rays telescope (XRT) from the space program of MPE/Garching provided a unique axion-ID potential for a helioscope like CAST. Recently, a 2nd 'small' XRT was attached to CAST magnet, which was constructed following the experience of the NuSTAR mission in USA. Also Micromegas detectors of various configurations are used in CAST at the extreme of lowest rates, reaching excellent performance. This pre-history is continuing in CAST. As next we expect a state-of-the-art force sensor and relic antennae, aiming to extend CAST's potential into the dark energy and to enter into the dark matter sector, respectively. Along with the experimental new ideas, CAST people with external collaborators proposed novel ideas, on which this proposal is based.

Dark energy: the greatest cosmic puzzle is still the dark energy, which manifests as the repulsive force ("antigravity") causing the increasing expansion of the universe. It makes most of the energy budget of the universe (~68%), but other than that, the nature and origin of this energy remain a complete mystery. Candidates for dark energy are either Einstein's cosmological constant or a "quintessence scalar field". The Chameleon field as a possible candidate for dark energy generates a 'fifth force' with a range inversely proportional to its "effective mass". If chameleons exist, they should be created also inside the Sun as they were first introduced in 2010 [1]. The present proposal to search for chameleons is the only one, which is based on real chameleon particles of solar origin, making it at least complimentary to all other chameleon searches. The very peculiar property of chameleon particles is their variable "effective mass", which depends on the ambient energy density. Inside a dense material, chameleons are (very) massive and therefore short ranged, while in vacuum or in outer space they become quasi massless. Because of its sensitivity on the environment, such a mass-changing scalar field has been named chameleon.

The pioneering search for solar chameleons via their coupling to photons (Primakoff-effect) has been performed by CAST [2], transforming thus CAST to the first chameleon helioscope! In the present proposal an upgraded InGrid detector [3] is aiming to optimize CAST's performance for this approach. Furthermore, a search for photon–chameleon–photon conversion has been performed, by other laboratory experiments like CHASE and ADMX, while OSQAR proposed recently a chameleon search, complimentary to this proposal, where a possible chameleon-fragmentation can be investigated. Interestingly, all these experiments, including CAST, were designed initially to search for axions.

Further, solar chameleons searches via their coupling to matter (and photons) have been suggestive for the present proposal. Chameleons always couple to matter, and under certain conditions they can be reflected off a denser material. While this peculiar property is familiar for photons, it is not obvious for other particles, and even less so for candidates from the dark sector; the underlying mechanism is completely different. This has important practical consequences for their detection: an XRT (or, in principle, any other telescope) becomes also a chameleon focusing / imaging device as it was suggested in [4], which is a "first" for the dark sector going beyond gravitational lensing. This is to be utilized in this proposal with a self-made sensitive force-sensor, developed initially in solid-state physics, providing a novel detection scheme via the "radiation pressure" expected from incident solar chameleons. It was first suggested in [5], using a prototype force sensor named KWISP being presently tested in INFN / Trieste. This detection scheme for solar chameleons has not been used before, at least not on purpose, and it is quite different from all other types of experimental chameleon searches. A different approach used by other experiments to test the chameleon mechanism involves small and unscreened test objects, like ultra cold neutrons and atomic

beams. A comparison between the various techniques is under investigation, and it might provide more insight into the experimental chameleon work.

Dark matter: Most laboratory, underground experiments and space missions are focused on the detection of massive WIMPs. The search for relic axions is by comparison very limited. And this, even though axions are theoretically introduced aiming to solve the strong CP-problem, which is a remaining fundamental problem for the Standard Model after the HIGGS discovery. Axions are also well motivated particles candidates for the mysterious dark matter in our Universe (~27% of its energy content). CAST is completing its search for solar axions or axion-like particles in 2015, and has the potential to open its horizon into this fascinating field. We propose to transform the powerful CAST dipole magnet to an antenna for dark matter axions or other relics with similar properties, using state-of-the-art new equipment as it was first suggested in [6]. This new possibility with CAST attracted the interest of a new collaborating Korean institute, but also people in CLIC, which are among the experimental pioneers in axion research [7], bringing thus the necessary expertise.

***In short*:**

a) After its recently pioneering search for solar chameleons, CAST has the potential to continue while being sensitive to both, their coupling to photons and to matter. Even though, they are not especially well motivated particles from the standpoint of fundamental physics, they are postulated candidates for dark energy, which presents such a profound mystery. CAST's large throughput XRT allows for a ~100x signal amplification combined with an unambiguous signal ID, and

b) CAST is aiming to transform its powerful dipole magnet to an antenna for dark matter axions, reaching eventually the line of the QCD inspired axions.

This is an ambitious well motivated research program, for which CAST people have the expertise, while continuing attracting people with appropriate expertise and state-of-the-art equipment like XRTs, Ingrid and KWISP. By comparison with other experiments in the field, the required resources are rather modest justifying CAST to enter deeper into the fascinating field of dark energy and dark matter, with a potential for a historical discovery.

References

[1] P. Brax, K. Zioutas, Phys. Rev. D82 (**2010**) 043007; arXiv:1004.1846v1 .

[2] V. Anastassopoulos, *et al*, (The CAST collaboration), *Search for chameleons with CAST*, Phys. Lett. B (**2015**) ; arXiv:1503.04561v1.

[3] C. Krieger, J. Kaminski, K. Desch, "*InGrid-based X-ray detector for low background searches*", Nucl. Instr. Meth. A **729** (2013) 905.

[4] K. Baker, A. Lindner, A. Upadhye, K. Zioutas, *A chameleon helioscope*, arXiv:1201.6508v1 (**2012**).

[5] S. Baum, G. Cantatore, D.H.H. Hoffmann, M. Karuza, Y.K. Semertzidis, A. Upadhye, K. Zioutas, *Detecting solar chameleons through radiation pressure*, Phys. Lett. B739 (**2014**) 167**; arXiv:1409.3852v2.**

[6] O.K. Baker, M. Betz, F. Caspers, J. Jaeckel, A. Lindner, A. Ringwald, Y. Semertzidis, P. Sikivie, K. Zioutas, *Prospects for searching axion-like particle dark matter with dipole, toroidal, and wiggler magnets*, Phys. Rev. D85 (**2012**) 035018; arXiv:1110.2180v1.

[7] W.U. Wuensch, …, Y.K. Semertzidis, …, *Results of a laboratory search for cosmic axions and other weakly coupled light particles*, Phys. Rev. D40 (**1989**) 3153; http://dx.doi.org/10.1103/PhysRevD.40.3153 .

2. InGrid-Detector for Chameleon/ALPS search - (responsible K. Desch)

2.1. Motivation

There exist only very few particle physics approaches to explain Dark Energy. The observed accelerated expansion of the Universe may be explained by the existence of a scalar field. One such scenario is the so-called chameleon for which a low-energy effective theory has been formulated [1]. Chameleons, like axions and other ALPS can created via the Primakoff effect in strong electro-magnetic fields present in the Sun and observed on Earth through the helioscope technique: ALPS with an effective coupling to electro-magnetic fields can be converted back into detectable photons within a strong magnetic field through the inverse Primakoff effect. The energy of the photons is practically identical to the thermal energy of the ALPS at the time of their Primakoff production in the Sun thus being in the soft X-ray regime. While axions may be created in the core of the Sun with a spectral maximum at approximately 3 keV, chameleons would be created in the solar tachocline [2] around 0.7 $R_{\odot}$ where intense magnetic fields are present. Thus they are produced at lower temperature corresponding to spectral maximum of only 600 eV (see Figure 2.1).
The CAST experiment has set the strongest limits on ALPS with axion-like couplings using low-background Micromegas detectors as well as a CCD detector mounted in the focal plane of an X-ray telescope behind the magnet [3]. These results are limited by the achievable background level (~ 10^{-6} counts/cm^2/s for Micromegas and ~10^{-4} counts/cm^2/s for the CCD detector [4]) and by the available observation time. Both Micromegas and CCD have a lower limit on the detectable photon energy around 1-2 keV rendering them barely efficient for the detection of converted chameleons.

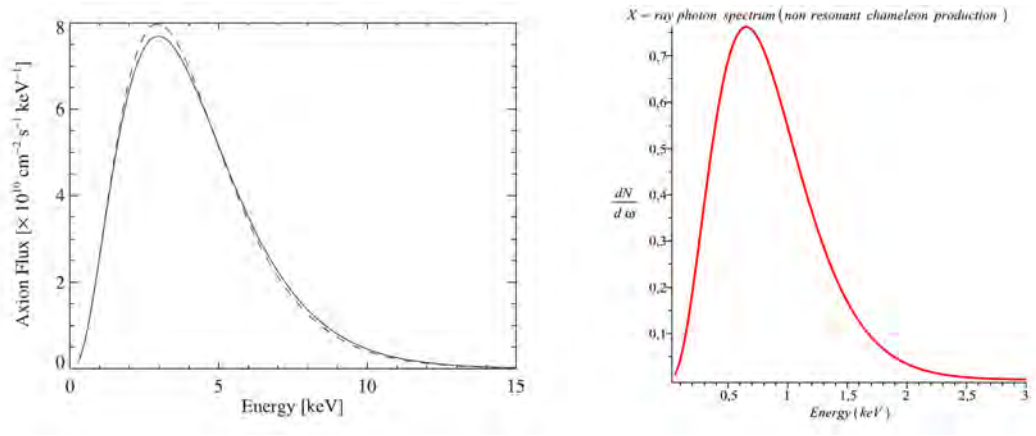

Figure 2.1 - Energy spectrum of solar axions (left) [3] and solar chameleons (right) [2].

An InGrid detector [5] has successfully been commissioned in a proof-of-concept run in CAST in 2014 and will be employed in 2015 to perform a solar chameleon search.
The aim of this proposal is to continue the search for solar chameleons and similar ALPs using an InGrid detector in 2016 and to observe evidence for such new particles or improve the world-best limit on the chameleon-photon coupling (expected from the upcoming 2015 InGrid run) production by a factor two (corresponding to a factor eight in the observable photon flux from converted chameleons). This is achievable through a combination of additional observation time and several improvements of the setup in order to further reduce background and increase detection efficiency in particular in the sub-keV regime.

2.2. **Status of detector and 2014/2015 data taking**

The InGrid detector (see Figure 2.2) is a gaseous ionization detector, which combines the Micromegas technique of gas amplification with an extremely granular 2D readout plane. The readout plane is realized as a CMOS pixel readout chip onto which the Micromegas amplification grid is mounted via wafer post-processing techniques. With a readout granularity 55×55μm^2, every single drifting electron can be detected and counted with almost 100% single-electron efficiency. The main advantages of this technique are:

1. the availability of "noise-free" measurement of the photon energy from counting the number of electrons created from the photo-electron. This energy measure is free if gas-gain fluctuations and electronic noise;
2. Soft X-ray photons can be detected down to very low energies (in principle down to the ionization threshold of about 25 eV, practically down to about 100 eV);
3. The possibility of a „topological" suppression of background from charged particles by identifying their track-like signature at scales as low as few hundred μm (s. Figure 2.3).

The detector consists of a conversion volume with a low electrical drift field. Electrons, originating from atoms ionized by radiation, drift towards the anode. Here a grid structure is placed above the readout plane. A very strong electrical field is applied between the grid and the readout. Electrons entering this gap undergo gas amplification, and the readout chip collects the avalanche. We use the Timepix ASIC [6], which has 256×256 pixels with a pitch of 55×55μm^2. The bump-bonding pads are used as charge-collecting anodes, which are individually connected to charge-sensitive amplifiers and signal processing. To optimally match the mesh to this pitch, it is built on top of the ASIC by photolithographic post-processing techniques. This ensures an excellent alignment of the grid holes with the charge collection pad. Figure 2.2 shows an SEM picture of an InGrid detector with the grid partially removed for better visibility.

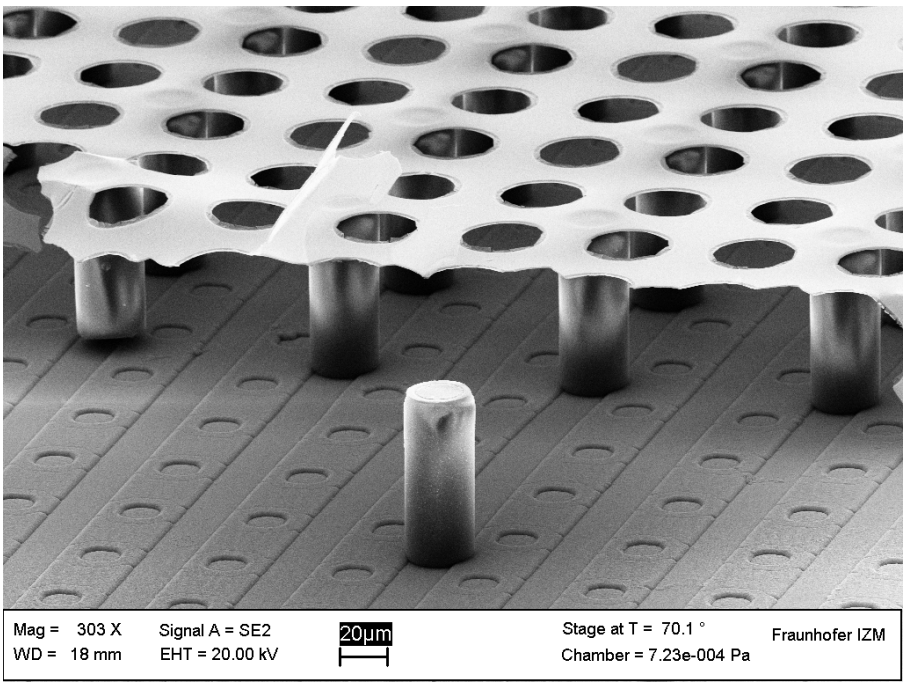

Figure 2.2 - SEM image of an InGrid [7]

If an electron enters the amplification gap, gas gains of 3000-5000 can easily be reached. The whole avalanche is collected by a single pixel operated typically at a threshold of 700 -1000 e^-, which allows for a very high detection efficiency of single primary electron. The chip records all pixels hit during a fixed time interval. Thus, even events consisting of a single primary electron could in principle be detected. Of course, it is not possible to distinguish such an event from rare noise or cross talk events, but according to first tests as few as three electrons seem to be enough to identify photons. Since an energy of about 25 eV is necessary to create an electron-ion pair, photons with energies of about 100 eV are detectable. Thus, the InGrid detector concept is very well suited to extend the physics potential of CAST to chameleon searches.

The UBonn group has significant experience with micro pattern gaseous detectors with highly pixelized readout. In the past years the group has concentrated on the advancement of InGrid detectors and their potential applications. In particular, the production process was transformed from experimental single-chip production to a more professional production on the wafer scale which yields about 100 InGrid detectors per production cycle [8,9]. This work has been carried out in close collaboration with Fraunhofer IZM in Berlin, NIKHEF in Amsterdam, the University of Twente, Netherlands and CEA Saclay, France. In parallel a new readout system was developed, which is based on the Scalable Readout System of the RD51 collaboration. The new readout system [7] allows for a high degree of flexibility, which is important for this project.

The group has performed extensive R&D work to characterize and improve the detectors. In a first master thesis [10,11] we studied the discrimination power based on an event shape analysis. A background sample was created using random triggers and recording all activities in the detector during 1 s intervals. The event shapes were compared to event shapes of photons created by a ^{55}Fe-source and a likelihood-ratio was used to separate the possible X-ray events in a background sample from track-like events. In this way a background suppression of more than 120 was demonstrated. In a Bachelor thesis [12] the same data sample was used, but more advanced algorithms employing artificial neural networks and boosted decision trees were used and even higher separation powers could be demonstrated. In these studies charged particles could be efficiently rejected if they have traversed the detector either parallel to the InGrid plane or have an inclination below a certain limit. For tracks passing almost perpendicular through the InGrid, the signal has a round shape and cannot easily be distinguished from X-rays anymore. To overcome this limitation the time development of the signal must also be recorded and analyzed, since in the case of perpendicular tracks, a significantly longer signal is expected. First tests in a master thesis [13] decoupled the signal from the aluminum mesh and recorded it with an FADC. This shows promising results, but more work is needed for a final application in CAST, in particular a high bandwidth preamplifier needed to drive the signal over the cable to the FADC must be redesigned and different signal shapings tested. It is planned to commission the mesh signal readout later in 2015 and fully exploit it in 2016.

The use of InGrid detector to be operated in the XRT focal plane was proposed in 2012 and the UBonn group joined the experiment in 2013. In 2013 and 2014 further tests of the detector were carried out in the context of CAST. First, the response to soft X-rays was characterized in the CAST Detector Lab (CDL) at CERN using the flexible X-ray gun with lines available in a broad energy range, down to the Carbon K_α line at 277 eV, which was observed clearly with the InGrid detector (see Figure 2.4). In 2014, a proof-of-concept experiment in the CAST setup was carried out. The InGrid detector, equipped with a 2 μm thick Mylar entrance window was placed into the XRT line of CAST and a first data set of 1 month including 27 sun trackings of 1.5h each could be taken. Smooth detector operation

could be demonstrated and preliminary data analysis already shows promising background levels (~3×10^{-4}/cm^2/keV in the 200-1000 eV range and ~10^{-5} in the 5-6 keV range) (see Figure 2.5). In another proof-of-concept experiment [14], CAST studied the possibility to gain sensitivity to solar chameleons using a Silicon Drift Detector. While a first limit could be set, we expect a significantly higher sensitivity with the InGrid detector due to the superior background reduction and the operation in the focal plane of the XRT.

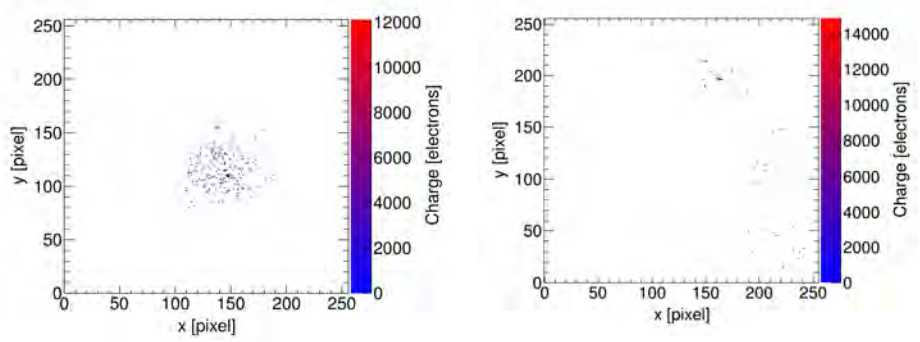

Figure 2.3 - Event display of a converted photon of ~5.9 keV *(Left), and* of a cosmic track (right).

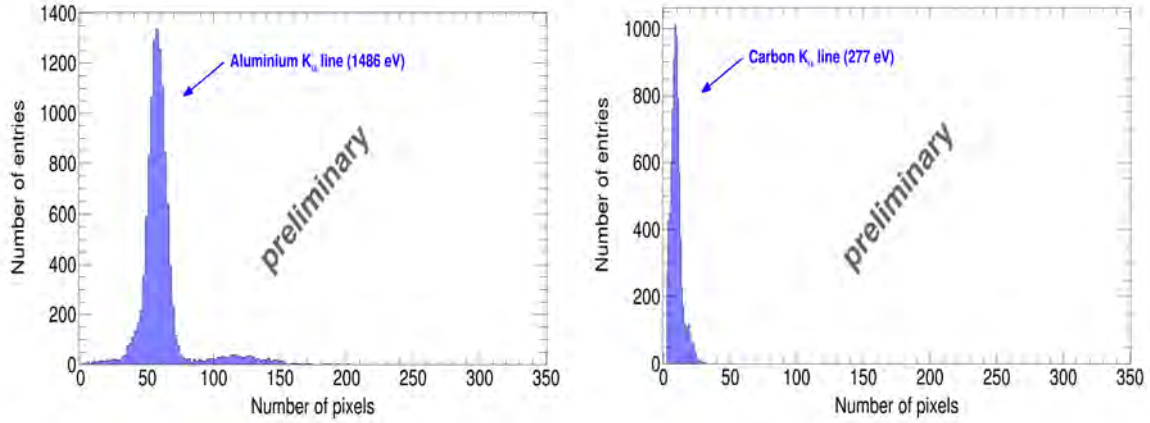

Figure 2.4 - InGrid detector test in the CAST detector lab: signals from two different X-ray lines.

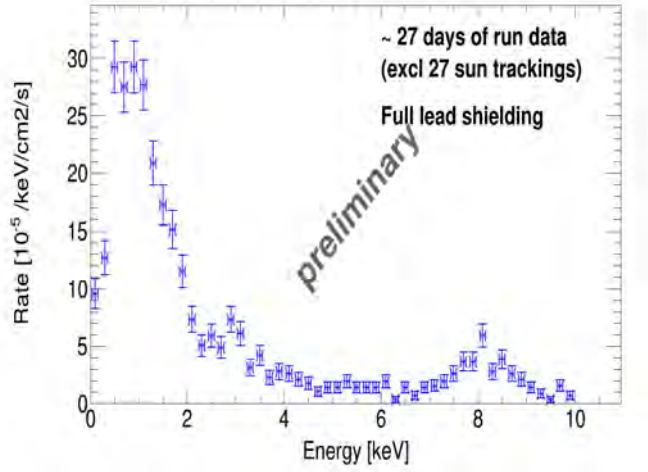

Figure 2.5 - Preliminary background spectrum of the InGrid detector in the 2014 test run in CAST

Meanwhile (May 2015) the InGrid detector was recommissioned in the XRT focal plane and is continuously taking background data and ready to take solar data as soon as the magnet is

cooled down. During the course of the 2015 run we intend to install two major improvements to further reduce background levels: the aforementioned readout of the mesh signal and an active cosmic muon veto using an external scintillator detector. Since these improvements will not be installed at the beginning of the run, their full potential can only be explored in a successive run in 2016.

2.3. Proposal to operate InGrid in CAST in 2016

We propose to operate the improved InGrid detector to fully exploit its discovery potential for solar chameleons through the chameleon-photon coupling in 2016.

Expected sensitivity
The extended sensitivity w.r.t. 2015 results from a combination of

- increased efficiency at sub-keV energies through the use of an ultra-thin ceramic window
- further background reduction through mesh signal readout
- further background reduction through scintillator veto
- additional observation time

Further improvement of background reduction may come from using a Timepix3-based InGrid which offers a 3-dimensional reconstruction of the charge cloud (micro-TPC). However it cannot be guaranteed that a Timepix-3-based InGrid will be available by the end of 2015.
As a sensitivity measure, we estimate the expected limit on the effective chameleon-photon coupling, β_γ. The estimation is based on simple scaling assumptions for exposure time, background level, accepted photon flux and detection efficiency as compared to the SDD measurements. In Figure 2.6, the estimated improvement of the expected limit on β_γ is shown. The estimate for the 2015 detector is based on a factor 10 longer observation time, a factor 16 larger flux due to the use of the XRT, a factor 10 lower background and a factor 3 worse efficiency due to the X-ray windows compared to the SDD result (blue box). For the improved detector to be operated in 2016, another factor 20 in background reduction, a factor 2 in efficiency and a factor 2 in observation time are assumed. The proposed detector thus has the potential to improve the sensitivity on β_γ roughly by a factor five w.r.t. the SDD measurement or a factor two w.r.t. to the most optimistic 2015 sensitivity.
It can be seen that the InGrid detector with the XRT setup has the sensitivity to surpass the solar limit (from sun cooling due to chameleon radiation) and produce the world-best limit on β_γ. In order to achieve the required background suppression, data analysis has to be developed further. In particular the low energy regime requires more elaborate techniques, since the low number of primary electrons allows for stronger variations in the parameters of interest and thus strong cuts are not possible. Overdetermination of various parameters such as energy and time development is important to give stronger handles for discriminating the background.

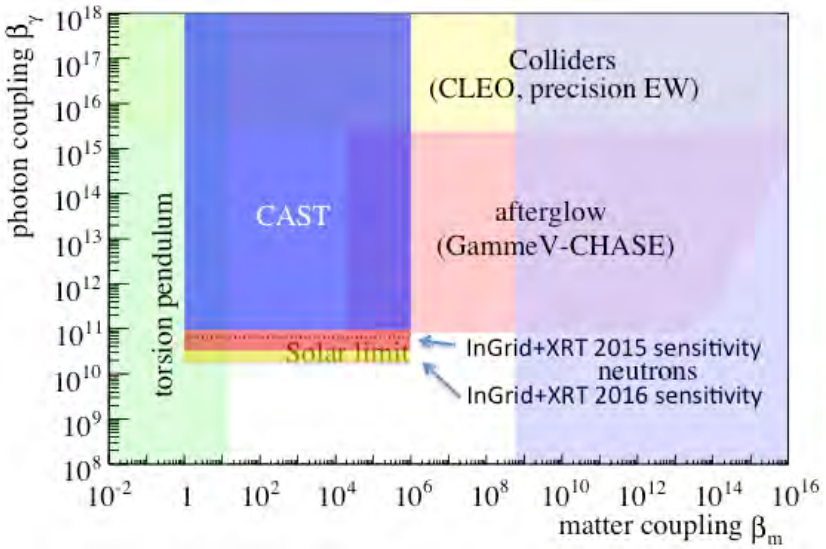

Figure 2.6 - Estimated sensitivity of the InGrid detector on the chameleon-photon coupling.

Higher sensitivity for low-energetic photons and improved energy resolution

While the detector itself is sensitive to broad range of X-ray energies as described above, the experimental setup requires vacuum in the X-ray telescope and 1 bar gas pressure in the detector. To achieve such a huge pressure difference, a differential pumping scheme has to be implemented requiring two thin windows. These windows have a finite transparency for low energetic X-ray photons. In Figure 2.7, the transparency of the entrance window for the currently used detector (2 μm Mylar foil metalized with 40 nm of aluminum) together with other options. To reduce the effective energy threshold of the detector, new material for the window, which can withstand a 1 bar pressure difference is needed. In particular, the sensitivity to chameleons can be significantly enhanced if a decent transparency below 1 keV can be achieved. A candidate material is a down to 200 nm thin structure of Silicon Nitride which we intend to study together with industry.

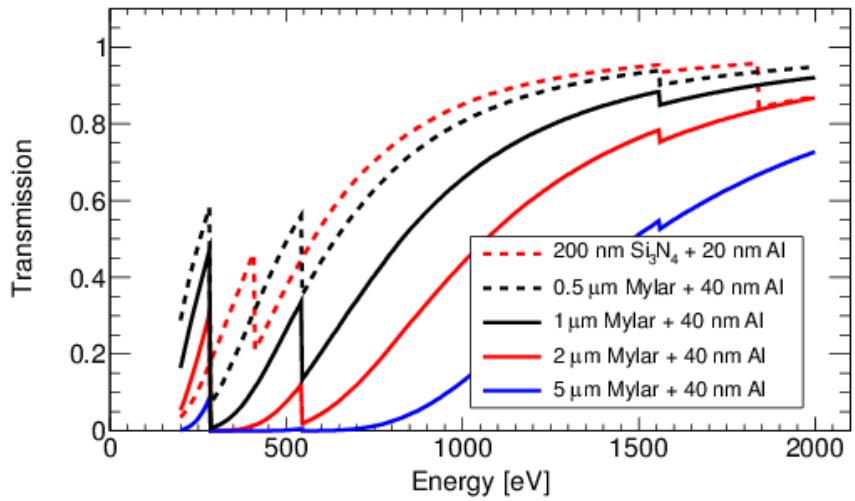

Figure 2.7 - Transparency of various windows.

As an interesting by-product we intend to perform measurements of the achievable energy resolution in this sub-keV energy regime which allows for a measurement of the Fano factor, which is not very well known in this energy regime.

Reduction of background

The largest fraction of the remaining background is caused by cosmic rays passing perpendicular to the InGrid through the detector and leaving a circular pattern of hit pixels indistinguishable from an X-ray photon signal. Additionally, cosmic rays can excite fluorescence radiation from the detector material. To reduce both effects two improvements can be implemented on a short time scale: The time development of the signal must be recorded. The difference in this quantity between an X-ray signal and track signal is significant as explained above. The second approach to suppress the cosmic ray background is to detect tracks by an external detector such as a scintillator and to remove events, where a track has passed through the InGrid (cosmic veto). Both ideas shall be implemented in the course of 2015. In addition to these two ideas, two longer term studies will be done to improve the radio-purity of the detector. Studies performed in Zaragoza have shown, that the standard FR4-based PCB contains a significant amount of radioactive elements such as ^{228}Ac, ^{212}Pb, ^{212}Bi, ^{214}Pb and ^{214}Bi (50-60 mBq each, per chip carrier). These can be avoided by designing a Kapton-based chip carrier. In addition, the remaining detector components (the drift cylinder and the cathode) can be adapted to the same high radio purity design implemented already in the Micromegas detectors of CAST. Alternatively, we intend to test the novel idea of producing these parts also from scintillating material and reading it out with a wavelength shifting fiber and Silicon Photomultipliers. Since the scintillating material is mostly made of plastic, it should have a very low natural radioactive contamination and the same argument holds for the drift cylinder and the cathode shielding as stated above for the small scintillator below the active area of the InGrid: If a charged particle passes through the scintillator shielding, the event can be removed from the analysis and no contamination of the data sample is possible. In this case a coincidence of several detector parts will produce a more reliable discrimination.

Depending on the progress in obtaining InGrids based on the successor chip of the Timepix, i.e. the Timepix3 chip, we will also address the use of a Timepix3-based detector within this proposal. There are important advantages of this chip over its predecessor: It can record both arrival time and charge of the signal for each pixel, the noise level of each pixel is reduced from 90 e^- ENC of Timepix to 60 e^- ENC of Timepix3, and the readout speed is significantly higher, reducing the dead time.

References

[1] J. Khoury and A. Weltman, "Chameleon fields: Awaiting surprises for tests of gravity in space", Phys. Rev. Lett. **93** (2004) 171104 [astro-ph/0309300]; J. Khoury and A. Weltman, "Chameleon cosmology", Phys. Rev. D **69** (2004) 044026 [astro-ph/0309411]; P. Brax, C. van de Bruck, A. C. Davis, J. Khoury and A. Weltman, "Detecting dark energy in orbit - The Cosmological chameleon", Phys. Rev. D **70** (2004) 123518 [astro-ph/0408415].

[2] P. Brax and K. Zioutas, "Solar Chameleons", Phys. Rev. D **82** (2010) 043007 [arXiv:1004.1846]; P. Brax, A. Lindner and K. Zioutas, "Detection prospects for solar and terrestrial chameleons", Phys. Rev. D **85** (2012) 043014 [arXiv:1110.2583].

[3] S. Andriamonje *et al*. [CAST Collaboration], "An Improved limit on the axion-photon coupling from the CAST experiment", JCAP **0704** (2007) 010 [hep-ex/0702006]; S. Aune *et al*. [CAST Collaboration], "CAST search for sub-eV mass solar axions with ^{3}He buffer gas", Phys. Rev. Lett. **107** (2011) 261302 [arXiv:1106.3919].

[4] M. Kuster, H. Brauninger, S. Cebrian, M. Davenport, C. Elefteriadis, J. Englhauser, H. Fischer and J. Franz *et al*., "The X-ray Telescope of CAST", New J. Phys. **9** (2007) 169 [physics/0702188].

[5] M. Chefdeville, "Development of Micromegas-like gaseous detectors using a pixel readout chip as collecting anode", Ph.D. Thesis, Amsterdam University, Amsterdam , The Netherlands (2009); M. Chefdeville *et al*., "An electron-multiplying 'Micromegas' grid made in silicon wafer post-processing technology", Nucl. Instrum. Meth. A **556** (2006) 490.

[6] X. Llopart *et al*., "Timepix, a 65k programmable pixel readout chip for arrival time, Energy and/or photon counting measurements", Nucl. Instrum. Meth. A **581** (2007) 485.

[7] M. Lupberger (for the LCTPC-Collaboration), "The Pixel-TPC: first results from an 8-InGrid module ", 2014 JINST **9** C01033.

[8] T. Krautscheid, Y. Bilevych, K. Desch, J. Kaminski, C. Krieger, M. Lupberger, F. Müller, "Gridpix: Production and application of integrated pixel readouts", Nucl. Instr. Meth. A **718** (2013) 391.

[9] W.J.C. Koppert,..., J. Kaminski *et al*., "GridPix detectors: Production and beam test results", Nucl. Instr. Meth. A **732** (2013) 245.

[10] C. Krieger, J. Kaminski, K. Desch, "InGrid-based X-ray detector for low background searches", Nucl. Instr. Meth. A **729** (2013) 905.

[11] C. Krieger, "Construction and First Measurements of a GridPix-Based X-ray Detector", Master Thesis, Bonn, February 2012, http://www.lhc-ilc.physik.uni- bonn.de/ergebnisse/abschlussarbeiten .

[12] S. Schmidt, "Verbesserung der Untergrundunterdrückung eines neuen CAST-Detektors mittels multivariater Methoden aus TMVA", Bachelor Thesis, Bonn, September 2013, http://www.lhc-ilc.physik.uni-bonn.de/ergebnisse/abschlussarbeiten.

[13] A. Deisting, "Readout and Analysis of the Induced Ion Signal of an InGrid Detector", Master Thesis, Bonn, May 2014, http://www.lhc-ilc.physik.uni-bonn.de/ergebnisse/abschlussarbeiten

[14] V. Anastassopoulos *et al*. [CAST Collaboration], "Search for chameleons with CAST", arXiv:1503.04561.

3. The expected sensitivity on solar chameleons with the radiation pressure sensor.

(K. Zioutas)

New results from other experimental searches for chameleons have been published since the publication of [1]. In particular, strong limits on chameleon models have been reported from searches using atomic interferometry [2] and neutron interferometry [3]. The projected sensitivity of our experiment is compared with these results and fundamental physical differences between the detection techniques discussed.

We assume a chameleon potential of inverse power law form [1]

$$V(\phi) = \Lambda^4 + \kappa\, \Lambda^{4+n}/\phi^n \tag{1}$$

where ϕ is the chameleon field, Λ is the intrinsic mass scale of the potential and $\varkappa$ a dimensionless coupling. If $\Lambda = \Lambda_{DE} = 2.4\text{x}10^{-3}$ eV, the constant Λ^4-term in $V(\phi)$ plays the role of the cosmological constant, and chameleons become a Dark Energy model. However, for our purposes only the dynamical behavior of the chameleon is of interest, which is not affected by the constant term. Accordingly, we drop this term and absorb the coupling $\varkappa$ in a redefinition of the mass scale Λ. However, we should keep in mind that, if we want the chameleon to play the role of Dark Energy, the intrinsic mass scale must be of order of the Dark Energy mass scale Λ_{DE}. Demanding the dimensionless parameter $\varkappa = (\Lambda_{DE}/\Lambda)^{4+n}$ to be natural, we can identify the physically interesting portion of the parameter space for the redefined mass scale to be within a couple orders of magnitude of Λ_{DE}.

The coupling to matter and radiation of the chameleon gives rise to the effective potential

$$V_{eff} = \Lambda^{4+n}/\phi^n + e^{\beta_m \phi/M_{Pl}}\rho_m + e^{\beta_\gamma \phi/M_{Pl}}\rho_\gamma, \tag{2}$$

where M_{Pl} is the reduced Planck mass, β_m (β_γ) parameterizes the coupling to matter (photons), ϱ_m is the local matter density and $\varrho_\gamma = ¼\ F_{\mu\nu}F^{\mu\nu}$ the Lagrangian density of the electromagnetic field. The corresponding effective mass of the chameleon depends on the local matter density

$$m_{eff}^2 = (n+1)\beta_m\, \rho_m/M_{Pl}\, \phi_{min} \sim \rho_m^{(n+2)/(n+1)}, \tag{3}$$

giving rise to large effective mass in dense environments for $n > -1$ or $n < -2$, the so-called Chameleon effect. ϕ_{min} is found by minimizing the effective potential (2),

$$\phi_{min} = \left(\frac{n\Lambda^{4+n}M_{Pl}}{\beta_m \rho_m}\right)^{1/(n+1)}. \tag{4}$$

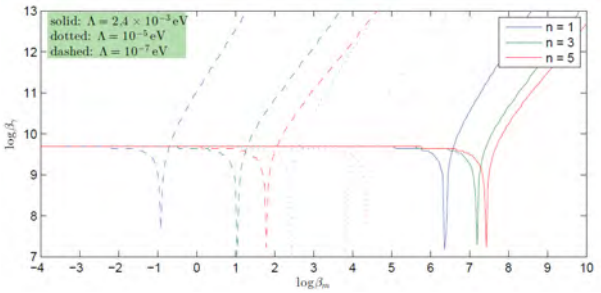

Figure 3.1 - Photon coupling β_γ, for which the chameleon luminosity L_{cham} is 4% of the total solar luminosity (L_{sol}), depending on the other chameleon model parameters β_m, n, and λ. From this, one can immediately calculate the chameleon luminosity for any other β_γ, since it scales as $L_{cham} \sim (\beta_\gamma)^2$.

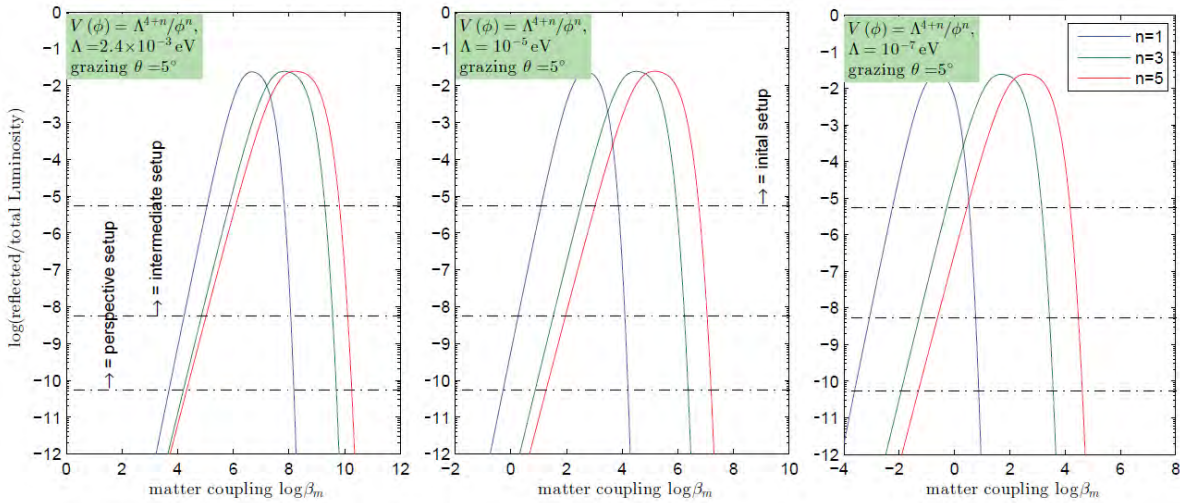

Figure 3.2 - Fraction of the total chameleon flux reflected by the force sensor membrane for a grazing angle of 5°. The chameleon potential mass scale is fixed to $\Lambda = \Lambda_{DE} = 2.4$meV (left), $\Lambda = 10^{-5}$eV (middle), and $\Lambda = 10^{-7}$eV (right), respectively. The horizontal black dash-dotted lines show the minimum fraction needed to detect chameleons, assuming $L_{cham}/L_{sol} = 4\%$. The upper line corresponds to the "initial" setup ($t_{meas.} =$ 100s and a flux enhancement by a factor 100 from an XRT). The middle line corresponds to the "intermediate" setup ($t_{meas.} = 10^4$s, a flux enhancement by a factor 100 from the XRT, and modulating the chameleon flux with a frequency of 2 kHz). The bottom line corresponds to the "perspective" setup ($t_{meas.} = 10^4$s, a flux enhancement by a factor 100 from the XRT, modulating the chameleon flux with a frequency of 2 kHz, and a sensitivity gain by a factor 100 from cooling the membrane). The corresponding value for β_γ can be read off Figure 3.1. For a β_γ of one order of magnitude smaller, this corresponds to shifting the horizontal dash-dotted lines upwards by two order of magnitude, since $L_{cham} \sim (\beta_\gamma)^2$. Note, that the β_m range differs between the plots.

Due to their coupling to photons chameleons will be produced in regions of high photon density. In the vicinity of an electric or magnetic background field the $\phi\gamma\gamma$ coupling phenomenologically turns into chameleon-photon mixing by the Primakoff effect. Hence, inside the Sun, where we have high photon densities and strong magnetic fields, chameleons will be produced, cf. the case for Axions. The predominant region of chameleon production in the Sun is the so-called tachocline, the thin transition zone between Sun's radiative core exhibiting almost solid rotation and the convective envelope rotation differentially. Here, the large shear causes strong magnetic fields. Such a chameleon flux can then propagate to the Earth and be discovered by the equivalence to radiation pressure: Chameleons cannot propagate in a medium if their effective mass within exceeds their total energy. Hence, they can be reflected by a sufficiently dense medium and be detected from their instantaneous momentum transfer to the medium.

The spectrum of solar chameleons, their propagation to the Earth, and the fraction of the chameleon spectrum which will be reflected by a force sensor in a suitable setup have been computed in [1]. Such an opto-mechanical force sensor, called KWISP for "Kinetic WISP detection", is being tested in INFN / Trieste. This sensor employs a 5x5mm^2, 100nm thick, Si_3N_4 nanomembrane (made by Norcada Inc., Canada, and having ϱ=3.2g/cm^3). It has recently been demonstrated to have a sensitivity of $S_{force,DC} \sim 10^{-14}$ N/Hz$^{1/2}$ for a continuous force on the membrane, and $S_{force,2\ kHz} \sim 10^{-16}$ N/Hz$^{1/2}$ if the incident pressure is modulated with a frequency of 2 kHz. The region of the chameleon parameter space accessible by such an experiment is revisited in the light of these numbers. As in [1], we assume a magnetic field of 30T in the tachocline extending about R_{tacho} = (0.70…0.75)xR_{sol}, where R_{sol} is the solar radius. As discussed in [1], the sensitivity of the sensor can be increased by employing an X-Ray

telescope (XRT), modulating the chameleon flux with a chopper, cooling the membrane, or coating the membrane with gold. As an "initial" setup we consider KWISP with the demonstrated force sensitivity for an unmodulated signal $S_{force,DC}$, employing the large XRT from MPE in CAST, and measuring for $t_{meas} = 100$ s, which is the time the sun is in the field of view of the XRT without moving it. With an aperture of $\sim$100 cm^2 and a spot size of $\sim$0.6 cm^2 for the XRT, we use a flux-enhancement factor of 100. As an "intermediate" setup we consider measuring for $t_{meas} = 10^4$ s and modulating the solar chameleon flux with a frequency of $f_{mod} = 2$ kHz using a chopper. As a "perspective" setup we assume gaining another factor 100 in force sensitivity from cooling the membrane to temperatures of the order of 10mK (see [1] and references therein), [4], on top of the "intermediate" scenario. The membrane is assumed to be mounted at grazing angles of $\theta=5^o$ and $\theta=10^o$ with respect to the incoming chameleon flux. We take into account lead-shielding upstream the sensor. The corresponding portions of chameleon parameter space are displayed in Figures 3.1, 3.2. The results are displayed in a different fashion in Figures 3.3-3.6 for ease of comparison with other experiments. The results are the same as presented in [1] but for the achieved sensitivity of the force sensor and for $L_{cham} / L_{sol} < 4\%$, where L_{cham} is the solar chameleon luminosity, and L_{sol} the total solar luminosity.

The features of the chameleon luminosity as well as the shape of the area of sensitivity have been discussed in [1]. We repeat a short discussion here: Considering the solar luminosity (Figure 3.1 and black regions of parameter space in Figures 3.3-3.6) the luminosity scales with $L_{cham} \propto \beta_\gamma^2$. For matter couplings β_m (and Λ, n) such that the effective mass of the chameleon is much smaller than the plasma frequency $\omega_{pl}^2=4\pi\alpha_{EM}n_e/m_e$ in the region of chameleon production, where α_{EM} is the fine structure constant, n_e the electron number density, and m_e the electron mass, the luminosity depends only on the chameleon-photon coupling β_γ and is about 4% of the solar photon luminosity for $\beta_\gamma \approx 10^{9.6}$. When the effective mass becomes of order of the plasma frequency the mixing angle becomes larger and one hits a resonance-like feature. Note that the exact shape of this resonance is not necessarily as shown in our plots: there our assumption that the mixing angle is much smaller than 1 does not hold up and our calculations are not reliable. Since this resonance if of no particular importance for this experiment, we did not investigate it further. If the exact form should become of interest, this region needs a more careful analysis. If one considers chameleon models even stronger coupled to matter, the luminosity decreases fast, because the effective mass of the chameleons in the tachocline becomes greater than typical photon energies there and hence, chameleons from photon-chameleon conversion cannot propagate anymore. The sensitivity of the sensor is centered around the resonance-like feature in β_m-space since both the position of the resonance and the region of sensitivity of the sensor are determined by the scaling of the chameleons' effective mass with ambient density. On the large β_m side, the sensitivity gets cut off because chameleons cannot propagate through the media upstream the detector, where the constraint comes from the assumed lead-shielding in our case. On the small β_m side, the sensitivity drops since chameleon models too weakly coupled to matter are not reflected by the membrane, and hence, a growing portion of the chameleon flux will pass through the membrane without momentum transfer.

Comparison with atom/neutron interferometry

Recently, new exclusion limits on chameleon models have been published from atomic interferometry [2] and neutron interferometry [3] experiments. Further limits for strongly coupled chameleon models come from experiments probing the quantum states of ultra cold neutrons (UCN) suspended above a mirror in the Earth's gravitational field [5]. The excluded parameter range overlaps with the portion of the parameter space a radiation pressure experiment would be sensitive to.

First, we would like to note that these experiments probe chameleon models fundamentally different to our radiation pressure experiment. Both type of interferometry experiments as well as the UCN experiment rely on the interaction of a test particle (neutrons or atomic nuclei) with a (classical) chameleon background field sourced by the close environment: In the case of the UCN-experiment the background field is sourced by the neutron mirror, in the case of the neutron interferometry experiment by a vacuum chamber the neutrons transverse, and in the case of the atomic interferometry experiment by an aluminum sphere mounted inside a vacuum chamber. In our radiation pressure experiment, we probe chameleon models through the interaction of "real" chameleons produced inside the Sun with a dense material on Earth.

Due to the fundamentally different ways of probing chameleon models the atom/neutron interferometry and UCN experiments are also not relying on the existence of any chameleon-photon coupling, while our radiation pressure experiment crucially relies on this coupling since otherwise no chameleons will be produced in the sun. However, as discussed in [1], and references therein, such a coupling is inevitable. While it is not generally agreed upon if it must be present at tree level, it is inevitably mediated by loops involving charged fermions. As an order of magnitude estimate we can thus assume $\beta\gamma \geq \alpha_{EM}^2\beta_m$, where $\alpha_{EM}\approx 1/137$ is the electromagnetic coupling. The published results from the interferometry and UCN experiments are displayed in Figure 3.7. Comparing the excluded portion of the chameleon parameter space, we note that our proposed radiation pressure experiment is sensitive to β_m well below the bound from neutron interferometry and gravitationally trapped neutrons. The parameter space these experiments exclude is not accessible by a solar radiation pressure experiment, since such chameleon models have either too large effective mass to be produced in the Sun's tachocline or will be absorbed by material between the Sun and the detector.

The bounds from atomic interferometry overlap with our region of sensitivity. However, our experiment has the potential to be sensitive to chameleon models with smaller matter coupling β_m. At the Dark Energy scale $\Lambda = \Lambda_{DE} = 2.4$ meV, [2] excludes $\log \beta_m \geq 4.7$ for $n = 1$ and $\log \beta_m \geq 5.3$ for $n = 5$. Our experiment is competitive already in the "initial" setup, being sensitive to matter couplings as small as $\log \beta_m \geq 4.9$ for $n = 1$ and $\log \beta_m \geq 5.8$ for $n = 5$ and will extend its reach in the "perspective" setup to $\log \beta_m \geq 3.5$ for n = 1 and $\log \beta_m \geq 4.1$ for $n = 5$. If we consider smaller energy-scales Λ, the comparison is even more in favor of our radiation pressure experiment: For $\Lambda = 10^{-5}$ eV, [2] excludes $\log \beta_m \geq 6.8$ for $n = 1,\ldots,5$ while our experiment is sensitive to chameleon models with matter couplings $\log \beta_m \geq 0.9$ for $n = 1$ and $\log \beta_m \geq 2.8$ for $n = 5$ already for the "initial" setup. For even smaller mass scales the atomic interferometry experiment loses its sensitivity entirely while our radiation pressure experiment becomes sensitive to chameleon models with even smaller matter couplings.

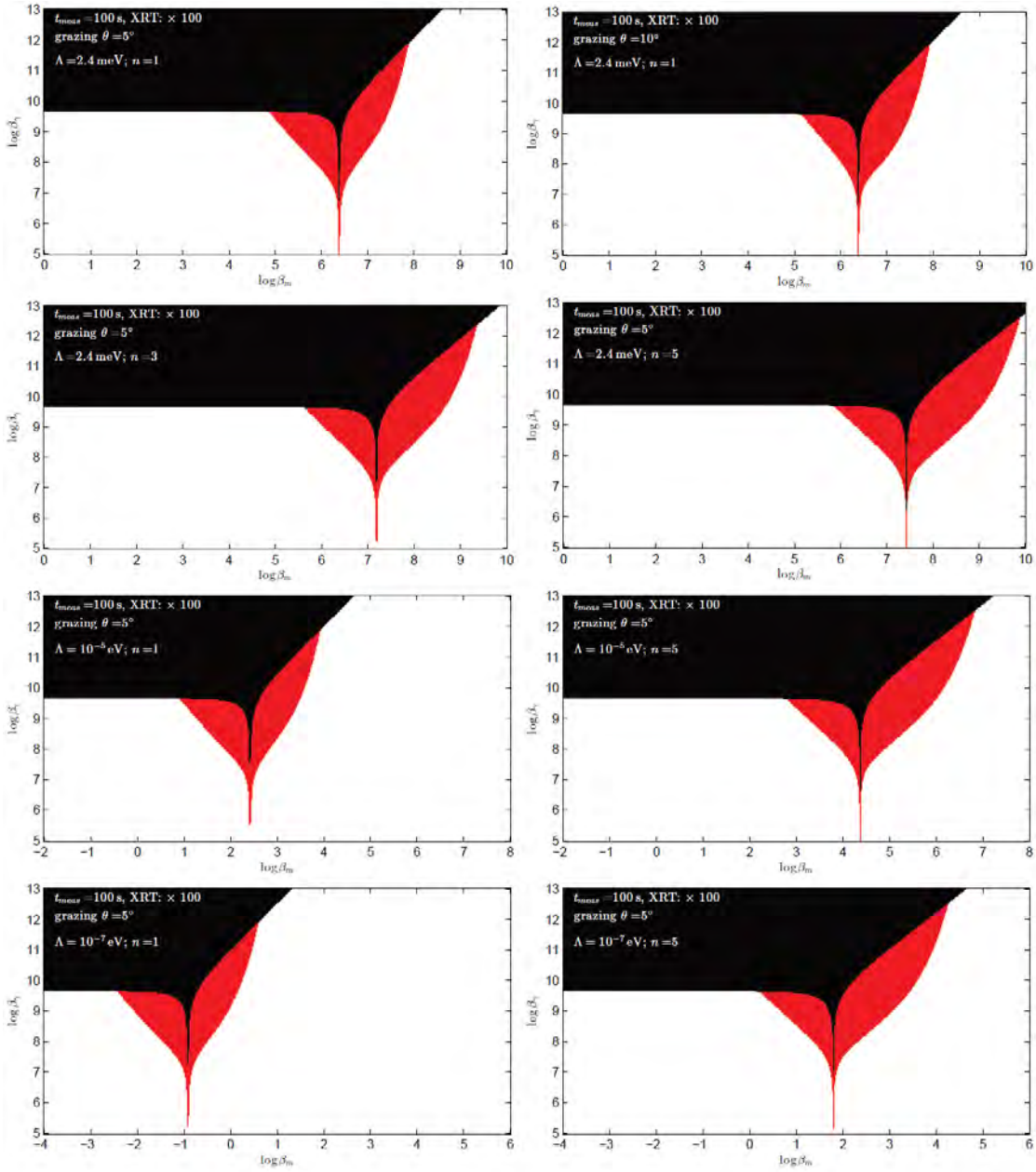

Figure 3.3 - Sensitivity plot of KWISP to solar chameleons in the β_m, β_γ plane. For the black portion of the parameter space the chameleon luminosity exceeds 4% of the total solar luminosity into photons, which is excluded by solar evolution. The red portion of the parameter space could be detected with KWISP in the "initial" setup ($t_{meas.} = 100$S and the XRT from MPE). The two top panels corresponds to $\Lambda = 2.4$meV, $n = 1$, and a grazing angle of $\theta = 5°$ (left) and $\theta = 10°$ (right). The second from top panels correspond to $\Lambda = 2.4$meV and $n = 3$(left), and $\Lambda = 2.4$meV and $n = 5$ (right). The third from top panels correspond to $\Lambda = 10^{-5}$eV and $n = 1$ (left), and $\Lambda = 10^{-5}$eV and $n = 5$ (right). The bottom left panel corresponds to $\Lambda = 10^{-7}$eV and □= 1, and the bottom right panel to $\Lambda = 10^{-7}$eV and $n = 5$. All but the top right panel are for a grazing angle $\theta = 5°$. Note that the β_m range differs between the plots for different Λ.

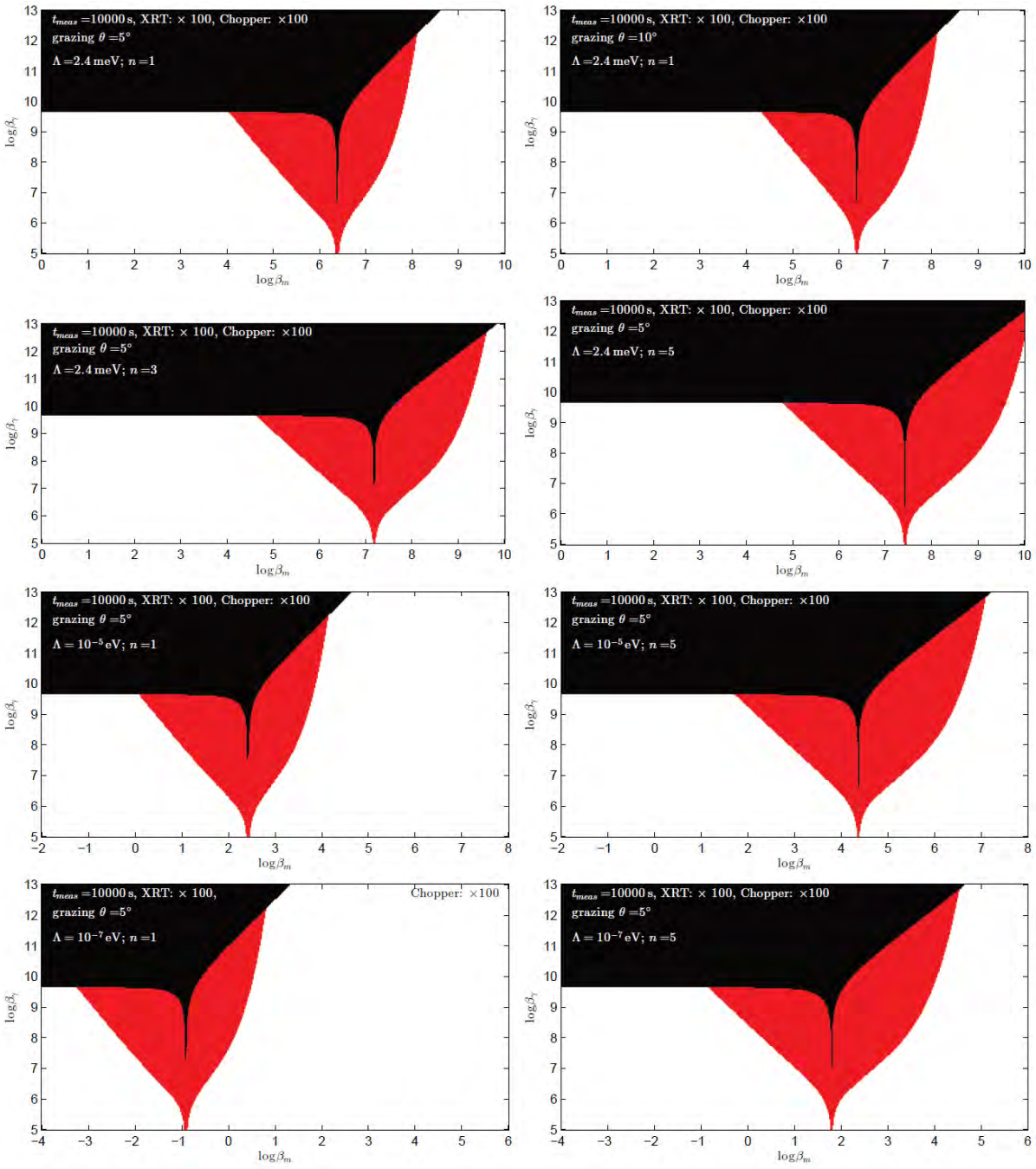

Figure 3.4 - Sensitivity of KWISP to solar chameleons in an intermediate setup with a flux enhancement from the XRT of 100, a modulation of the flux with 2 kHz, and measuring for $t_{meas.} = 10^4$s. The chameleon-model parameters corresponding to different plots are the same as in Figure 3.3.

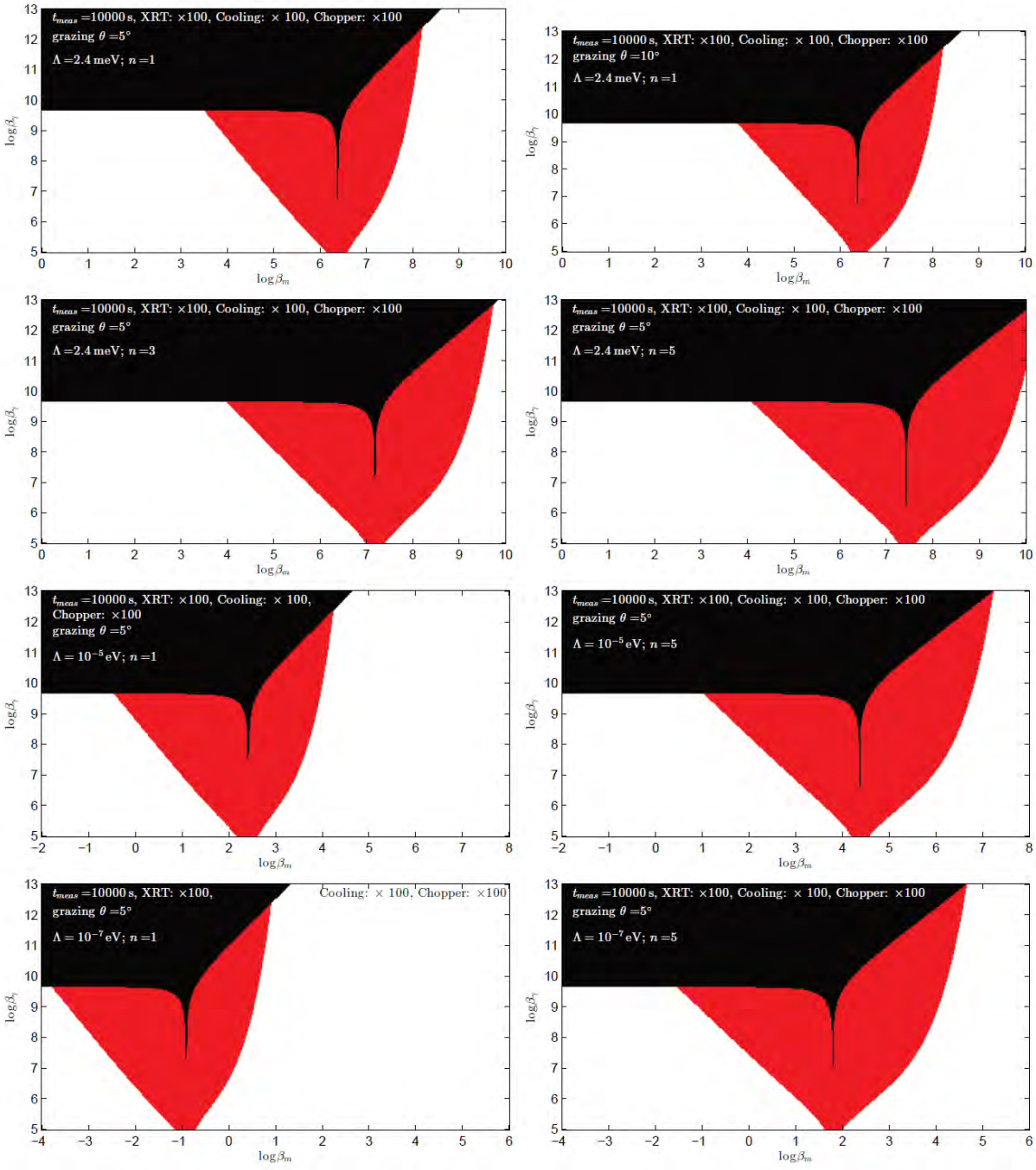

Figure 3.5 - Sensitivity of KWISP to solar chameleons in the "perspective" setup with a flux enhancement from the XRT of 100, a modulation of the flux with 2 kHz, cooling the membrane, and measuring for $t_{meas.} = 10^4$s. The chameleon-model parameters corresponding to different plots are the same as in Figure 3.3.

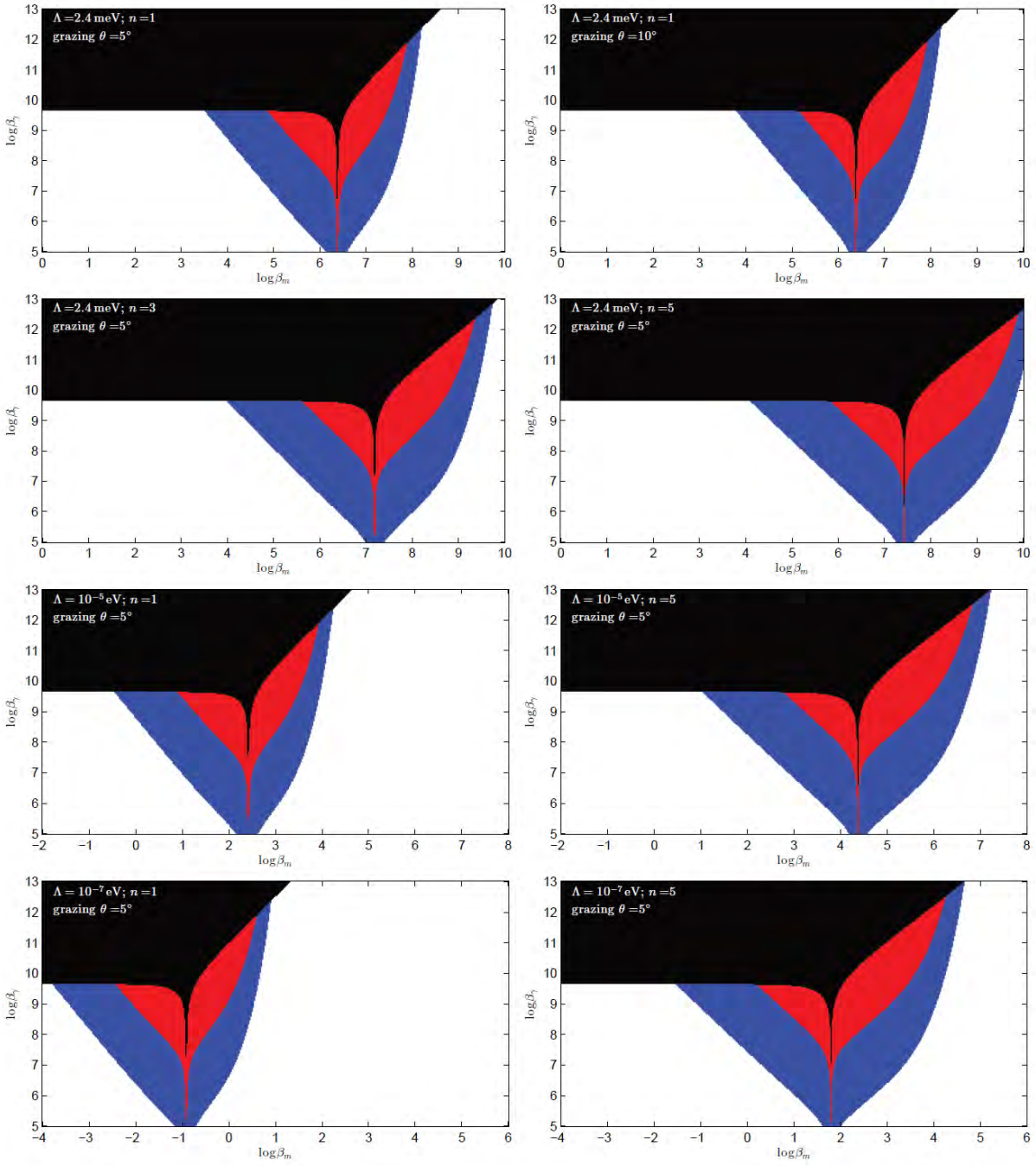

Figure 3.6 - Comparison of the sensitivity of KWISP to solar chameleons for the "initial" setup (red) and for the "perspective" setup (blue). The chameleon model parameters corresponding to different plots are the same as in Figure 3.3.

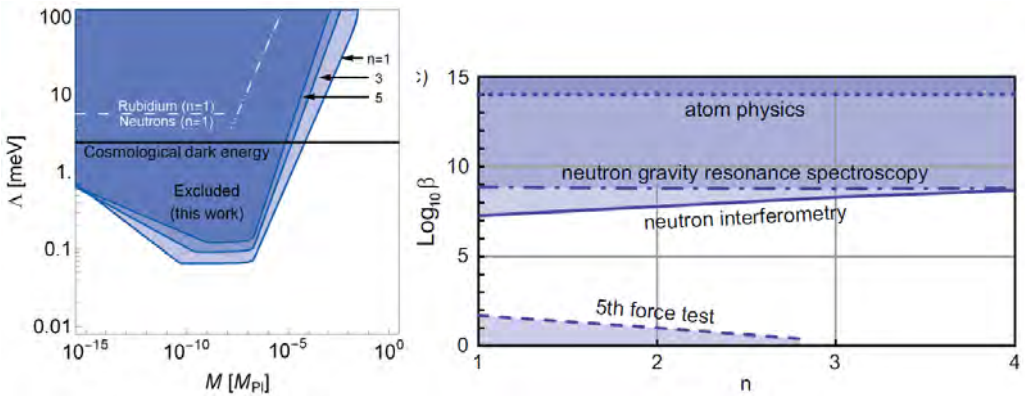

Figure 3.7 - Exclusion limits on chameleon models from atomic interferometry (left) and neutron interferometry and UCN (right, UCN result labeled "neutron gravity resonance spectroscopy"). In the left panel the definition of the intrinsic energy scale Λ agrees with our definition, while the matter coupling is parametrized by M, where for comparison to our definition $M/M_{Pl} \equiv \beta_m^{-1}$. In the right panel $\beta \equiv \beta_m$ and the plot is valid for the intrinsic mass scale $\Lambda = \Lambda_{DE} = 2.4\text{meV}$. The definition of n in both plots agrees with our definition. Plots taken from [2] (left) and [3] (right). The bounds from the UCN-experiment agree with the bounds published in [5]. Note, that the exclusion limit from UCN-neutrons extends to $n > 4$ with the bound on $\beta_m \leq 10^9$ nearly constant, cf. [5].

Conclusions

Chameleon models are among the leading candidates to explain the observed expansion of the Universe by Dark Energy. Thanks to the rich phenomenology of chameleon models, strong constraints can be made from "fifth force" searches like atomic/nuclear interferometry, probing the quantum states of ultracold neutrons in gravitational fields, Casimir force experiments or " $1/r^2$ " test like the Eöt-Wash experiment. However, they are an effective theory and the underlying fundamental mechanism is not understood as yet. This makes the need to probe such models by independent, physically different searches even greater.

We have revisited the sensitivity of a search for solar chameleons through radiation pressure proposed in [1] in the light of advances in the experimental realization of such an experiment. We have shown, that besides giving independent confirmation for bounds from other searches, a realistic setup can access uncharted chameleon model parameter space already in an "initial" setup. We also discussed realistic mid- and long-term improvements of the experiment's sensitivity, which can access a sizable portion of the unprobed chameleon model parameter space.

References

[1] S. Baum, G. Cantatore, D.H.H. Hoffmann, M. Karuza, Y.K. Semertzidis, A. Upadhye, K. Zioutas, Phys. Lett. B 739 (**2014**) 167; arXiv:1409.3852v2 [astro-ph.IM].

[2] P. Hamilton, M. Jaffe, P. Haslinger, Q. Simmons, H. Müller, J. Khoury, arXiv:1502.03888v2 [physics.atom-ph] (**2015**).

[3] H. Lemmel, P. Brax, A.N. Ivanov, T. Jenke, G. Pignol, M. Pitschmann, T. Potocar, M. Wellenzohn, M. Zawisky, H. Abele, Phys. Lett. B743 (**2015**) 310; arXiv:1502.06023v1.

[4] M. Karuza, C Molinelli, M Galassi, C Biancofiore, R Natali, P Tombesi, G Di Giuseppe, D Vitali, New J. of Physics 14 (**2012**) 095015; doi:10.1088/1367-2630/14/9/095015 .

[5] T. Jenke, G. Cronenberg, J. Burgdörfer, L.□A. Chizhova, P. Geltenbort, A.□N. Ivanov, T. Lauer, T. Lins, S. Rotter, H. Saul, U. Schmidt, H. Abele, Phys. Rev. Lett. 112 (**2014**) 151105; http://dx.doi.org/10.1103/PhysRevLett.112.151105.

4. **KWISP - Kinetic WISP detection** - Working Group* (Responsible G. Cantatore)

4.1. **Motivations and force-sensor detection principle**

We propose to install on CAST a novel type of sensor to detect the hypothetical flux of Chameleons produced in the sun by exploiting their local density-dependent direct coupling to matter [1]. The principle of the "kinetic detection" of chameleon-type WISPs is as follows. A flux of solar chameleons will exert the equivalent of a radiation pressure on a solid surface of appropriate density, such as a thin and rigid dielectric micro-membrane suspended inside a resonant optical Fabry-Perot cavity. The collective force exerted by solar Chameleons bouncing off the membrane surface excites its vibrational states and causes a displacement from its equilibrium position. When a laser beam is frequency-locked to the cavity by means of an active electro-optical feedback system, any membrane displacement from the initial position will cause cavity mode frequencies to experience a shift, which is then sensed in the feedback correction signal (see Figure 4.1). The sensor thus transduces displacement (force) into an electrical signal with an added gain proportional to the finesse of the Fabry-Perot resonator [2, 3].

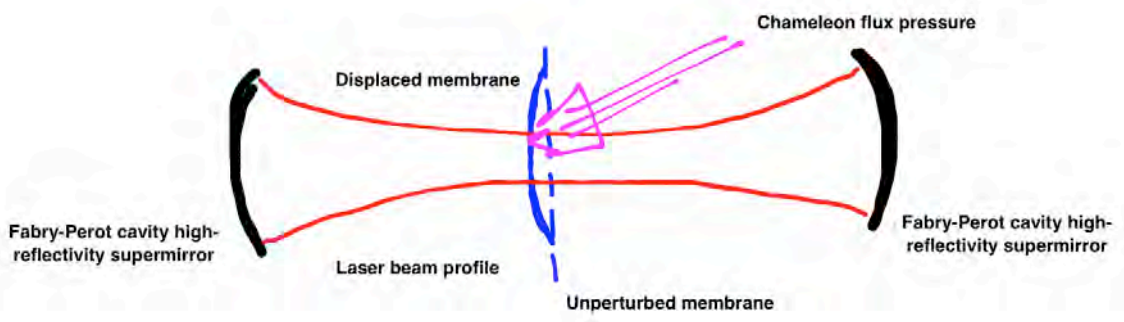

Figure 4.1 - Pictorial representation of the effect of a chameleon flux pressure on a micro-membrane inside a Fabry-Perot cavity (see also text).

This state-of-the-art opto-mechanical sensor (KWISP, for Kinetic WISP detection) will soon make CAST one of the very few experiments sensitive to Dark Energy candidate particles, and this search for matter coupling of solar chameleons has the potential to obtain new results in the field.

4.2. KWISP force sensor status

A prototype opto-mechanical sensor has been built and calibrated at INFN Trieste. It consists of a Si_3N_4, thin (50-100 nm), membrane with lateral dimensions of a few mm suspended inside a Fabry-Perot resonator cavity. The cavity is formed by two concave (curvature radius 1 m), high-reflectivity ($R < 99.999\%$), multi-layer dielectric mirrors with their reflecting surfaces placed face to face at a distance of 85 mm. The mirrors can be aligned by means of piezoelectric actuators and the membrane can also be moved in three linear dimensions and two angular ones, in order to align it and displace it along the cavity optical axis. The entire assembly sits in a vacuum enclosure with suitable viewports to admit a sensing laser beam at

* D. Hoffmann (TU Darmstadt), M. Karuza (U. Rijeka), Y. Semetrtzidis (CAPP), K.Zioutas (U. Patras and CERN)

1064 nm emitted by a CW Nd:YAG laser. This is necessary in order to avoid perturbations from the Brownian motion of the air (see Figure 4.2). The optics scheme of the KWISP sensor prototype is sketched in Figure 4.3.

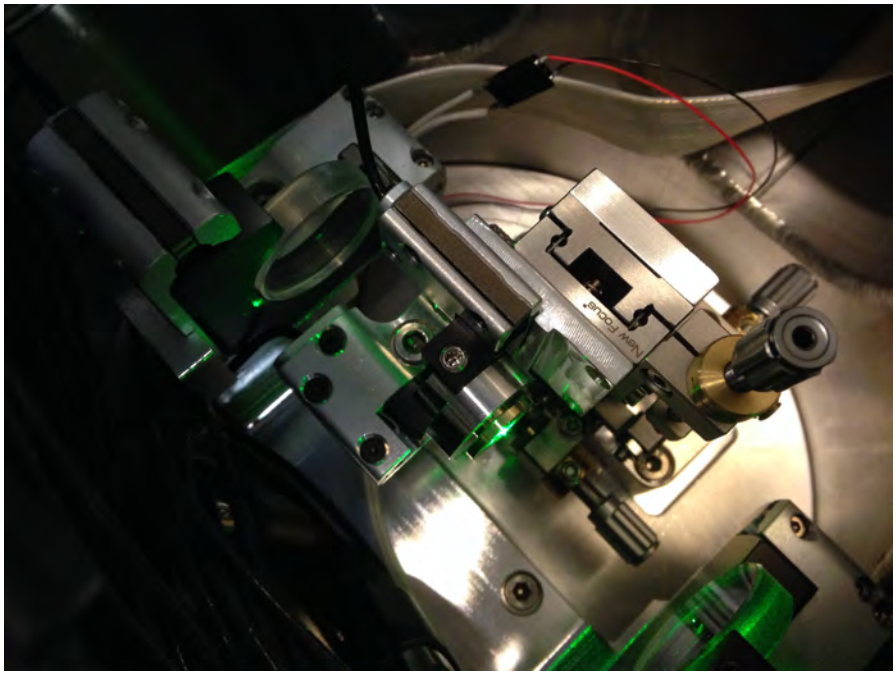

Figure 4.2 - Photograph of the interior of the KWISP force sensor vacuum chamber. A membrane holder is visible at center, and cavity mirrors are also visible at upper left and lower right.

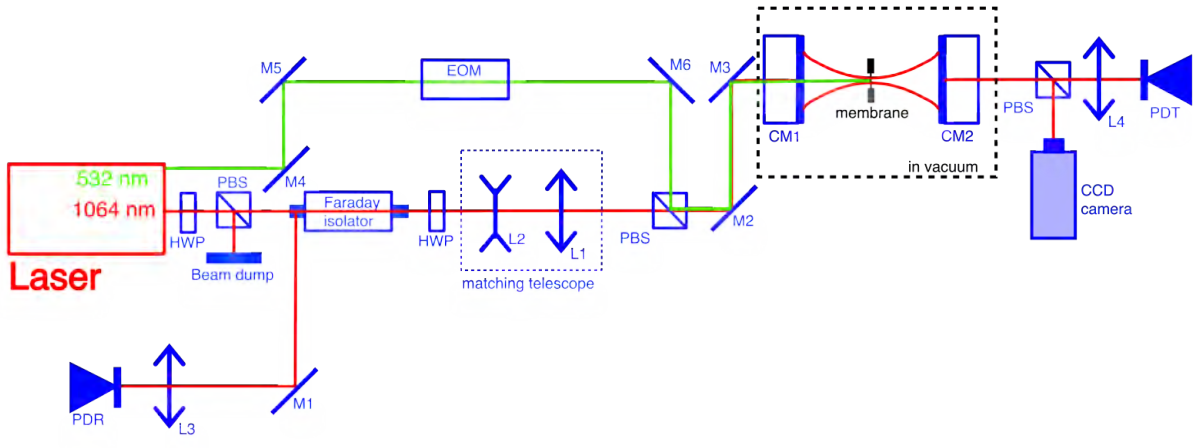

Figure 4.3 - Sample optics scheme of the KWISP force sensor prototype (see text)

During operation the optical resonator cavity is frequency-locked to the sensing laser beam using an electro optic feedback [2]. The feedback acts on the laser so that the instantaneous distance between the cavity mirrors, left "free" to float, is always a half-integer multiple of the laser wavelength. When the cavity is at resonance, its normal modes are not perturbed if the membrane, almost completely transparent to the laser wavelength, is aligned and positioned near a node of the standing intra-cavity electric field. A subsequent membrane displacement couples the membrane mechanical modes to the TEM modes of the cavity,

detuning mode proper frequency with a typical oscillatory dependence on membrane position along the cavity axis [4]. The sensor is calibrated by determining its detuning curve, which gives mode frequency shifts as a function of membrane axial displacement. Using the membrane mechanical characteristics, the curve can be expressed in terms of the force acting on the membrane. A finite-element modeling software has been used for this purpose.
Finally, to determine the sensor response to a given pressure signal, a second "pump" beam, at a wavelength different from that of the "sensing" beam and at which the membrane is reflecting, is directed at the membrane in order to excite it with a radiation pressure. The pump beam intensity is also time-modulated with a chopper in order to obtain a signal away from zero frequency, where most of the noise occurs.

4.3. Prototype calibration results

The KWISP force sensor was calibrated with a (5 mm)x(5 mm) 100 nm thick Si_3N_4 membrane inserted in the sensor optical resonator cavity (see Figure 4.4).

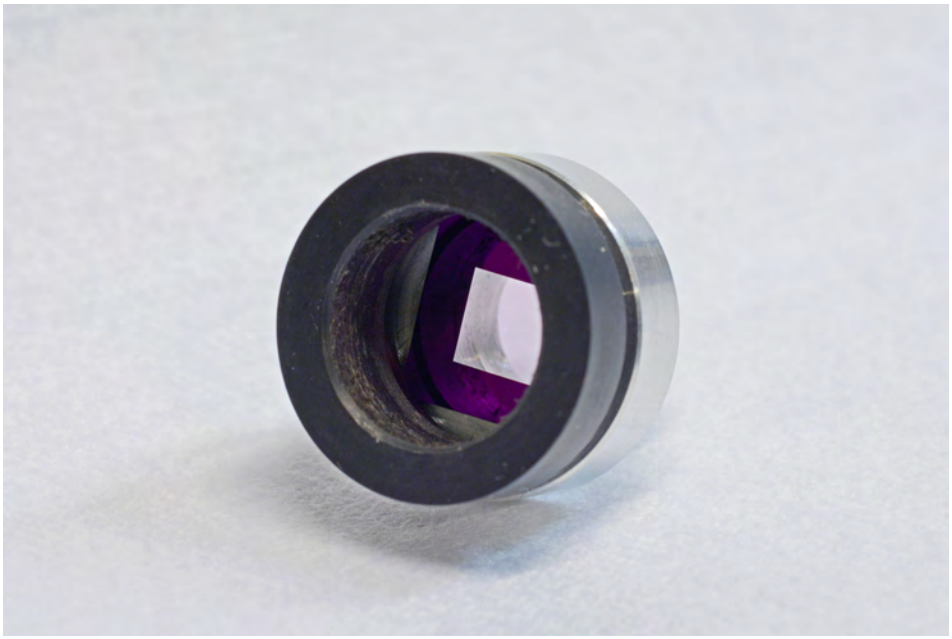

Figure 4.4 - Photograph of the (5 mm)x(5 mm) 100 nm thick Si_3N_4 membrane mounted on its holder and ready to be installed inside the Fabry-Perot cavity.

Recall that an external force causes a membrane displacement from its initial position the cavity, which is then detected by monitoring the cavity instantaneous resonant frequency. Membrane alignment was carried out first in air with a manual micrometric tilting stage, then in vacuum with a PZT-actuated second tilting stage, and with the help of an auxiliary 532 nm laser beam which, contrary to the main 1064 nm beam, is reflected by the membrane and can be used a guide for positioning. Proper alignment was achieved by observing the spatial shape and transmitted intensity of the cavity modes in the presence of the membrane.
To measure the sensor detuning curves one must obtain a plot of transmitted mode frequency vs. membrane displacement along the cavity axis. The plot shows, for each transmitted mode, how mode frequency changes with membrane displacement (“detuning”). The plot is

constructed by scanning membrane positions along the cavity axis, starting from an arbitrary initial position, and by recording, for each such position, the frequency at which a given mode resonates and is therefore transmitted by the cavity. The actual measurement is done using a LabView program, controlled by a PC and running on an FPGA board, which moves the membrane, scans the laser frequency and acquires the light intensity transmitted through the cavity. Data can be presented in a frequency-shift ("detuning" with respect to the main laser line) vs. membrane-displacement plot. Data points in this graph give the frequency at which a given mode resonates as a function of membrane position. A sample plot is shown in Figure 4.5 below, where a portion of the typical oscillatory dependence of the detuning on the displacement can be seen. If one selects a region where the slope is maximum, a linear fit to the data gives the transduction coefficient of the sensor in terms of frequency detuning response to a given membrane displacement.

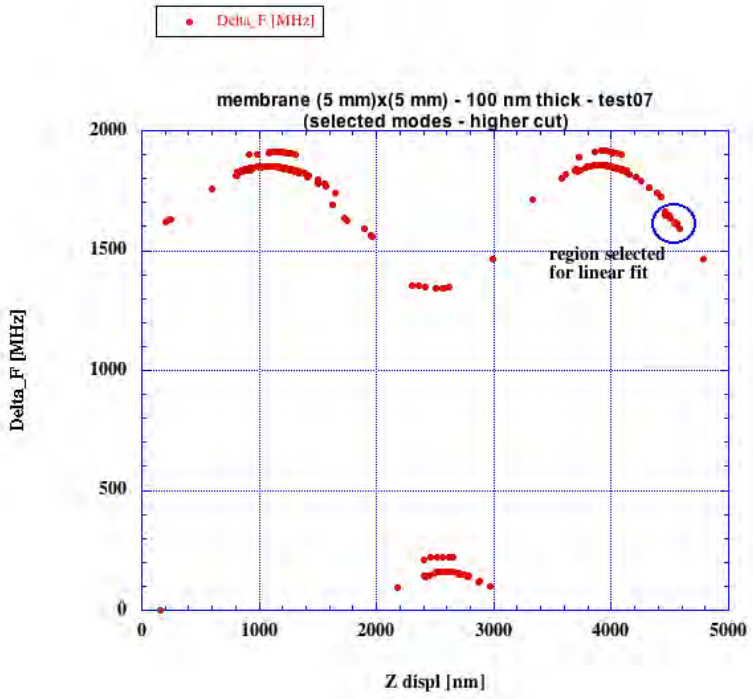

Figure 4.5 - Detuning curve of the KWISP sensor (see text). Most intense mode is shown. Data points in the circled region are used for the sensitivity estimate.

In the case represented in Figure 4.5 this slope corresponds to 0.426×10^6 Hz/nm or, in terms of force, 2.56×10^{13} Hz/N. This last value is derived from a finite elements analysis, carried out by A. Gardikiotis, yielding an equivalent spring constant of 16.6 N/m.
After measuring the detuning curves the 1064 nm laser beam was frequency-locked to the Fabry-Perot cavity (see Figure 4.6), and the relevant noise spectral density in the locking feedback loop was determined.

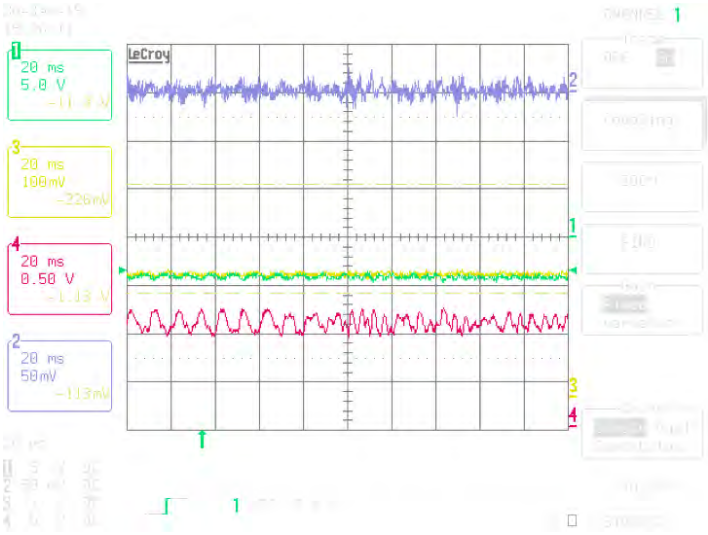

Figure 4.6 - Laser-cavity frequency locking: the red trace gives the light intensity transmitted through the cavity during lock. The membrane is present within the cavity. The light blue curve is the feedback loop correction signal from which one extracts the noise spectral density needed for sensitivity measurements (see also text).

This noise figure, combined with the characteristic coefficients deduced from the detuning curves, allow an experimental determination of the sensor displacement and force sensitivities (recall that displacement is translated into force by modeling the membrane with a finite elements analysis software yielding an equivalent spring constant).
Displacement sensitivity: 1.7×10^{-15} m/√Hz @ DC (4.2×10^{-17} m/√Hz @ 2 kHz)
Force sensitivity: 2.7×10^{-14} N/√Hz @ DC (7×10^{-16} N/√Hz @ 2 kHz)

A direct determination of the sensor response to an external exciting force was also carried out as a final performance test of the system. The external force is provided by the radiation pressure exerted by an auxiliary "pump" beam at 532 nm reflecting off the membrane (membrane reflectivity at 532 nm is about 20%). This beam is amplitude modulated at 9.045 kHz using an electro-optic modulator, in order to introduce a specific frequency at which one searches for the radiation pressure effect. When the auxiliary 532 nm beam is on and modulated, a peak at 9.045 kHz is observed in the power density spectrum of the error signal of the laser-cavity locking circuit. The laser light power at 532 nm reflecting off the membrane was 100 micro-W, corresponding to a radiation pressure of 1.75×10^{-8} N/m^2. Given the surface area of the 5x5 mm^2 membrane, the total force on the membrane itself was 4.4×10^{-13} N. Since the observed peak was a factor 30 above background, and taking into account the 1 Hz frequency resolution of the power spectrum, the resulting force sensitivity is 1.5×10^{-14} N/√Hz. This directly measured value compares well with the previous indirectly obtained estimated giving confidence in the performance of the sensor.

4.4. **Commissioning status and proposed activities at CAST**

The sensitivity demonstrated by the KWISP force sensor can be fully exploited in searches for solar chameleons at CAST. The MPE XRT installed on CAST acts also as a chameleon concentrator, and mounting the force sensor in or near its focal plane will grant an increase in the expected solar chameleon flux by a factor 100 or more. Also, the solar tracking capability of the CAST magnet carriage can be exploited to increase integration time, to conduct background runs when pointing off the sun, and to look for a specific time dependence of an eventual signal by keeping the sensor stationary while the sun apparently moves across it.
The commissioning of the KWISP sensor at CAST will be carried out in two phases.

In the first phase, which is already under way, the prototype tested in the Trieste laboratory is to be transferred to CERN. A duplicate setup will be kept in Trieste in order to preserve the capability of testing new components, planned upgrades and new ideas without interfering with the main sensor in operation at CERN. The KWISP prototype is being initially installed "off-beam" in the CAST area in order to validate its calibration and performance in the actual working environment. Preliminary vibration tests have already been carried out on the optical table prepared for these off-beam tests, finding that the mechanical perturbations are concentrated mostly below 1 kHz. This is highly encouraging, since the finite elements analysis of the membrane mentioned above finds for it a mechanical resonance frequency of ~354 kHz, with a quality factor of ~80000. This means that mechanical vibrations far from this frequency should be highly suppressed.
The second phase of the commissioning involves placing the force sensor in correspondence of the MPE XRT focal plane, running calibration and performance checks and taking preliminary solar data (Figure 4.7). A custom vacuum chamber to hold the membrane-cavity assembly is now in the design phase, with special attention at minimizing the interventions necessary to install it on the MPE XRT beamline (Figure 4.8). The optics scheme will be modified with respect to the off-beam prototype in order to take advantage of optical fiber transport of the primary laser beam from the off-beam optical bench to the membrane-cavity assembly. A 40 m long optical fiber is already in place connecting this bench to the MPE XRT beamline.

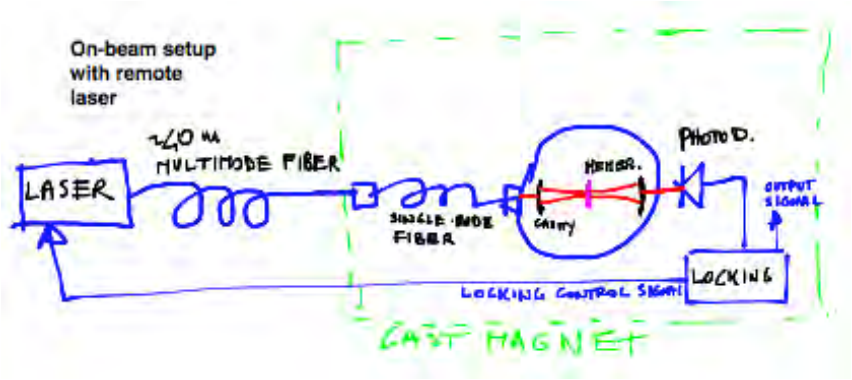

Figure 4.7 - Sketch of the on-beam setup of the KWISP force sensor

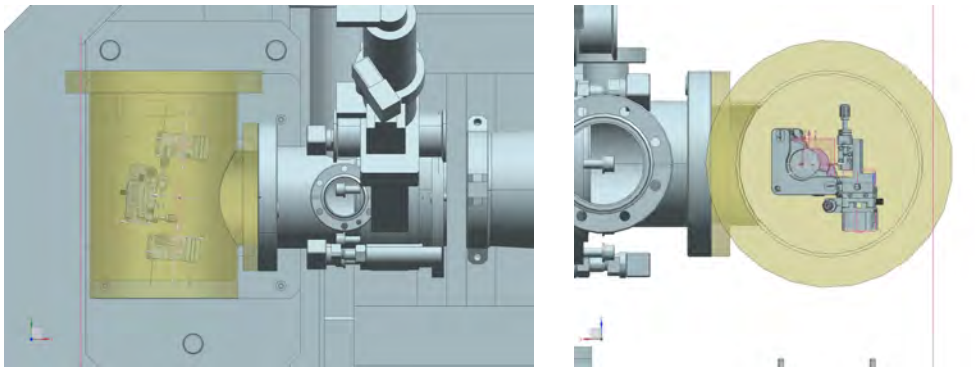

Figure 4.8 - Draft CAD design of the on-beam KWISP vacuum chamber (INFN Trieste)

Calibration and sensitivity checks can start once the force sensor is in place on-beam. In fact, sensitivity measurements may also serve as preliminary "physics" runs: if the prototype

measured sensitivity is confirmed, the measurement time needed to achieve a "first" result is very short, of the order of 100 s.
Upgrades can be applied to the KWISP force sensor to increase the physics reach of CAST in the dark energy sector. Short-medium terms upgrades involve the use of a chopper and a new detection scheme based on the principle of homodyne detection. These techniques could increase the sensitivity by a factor 100-1000. An additional factor 100 could be gained in the longer term by cooling the membrane, either with cryogenic of with optical techniques, down to ~K temperatures.

References

[1] S. Baum et al., Physics Letters B **739**, 167–173 (2014)
[2] G. Cantatore et al., Rev. of Sci. Instr., **66(4)** 2785–2787 (1995)
[3] M. Karuza et al., J. Opt. **15**, 025704 (2013)
[4] M.Karuza et al. New J. of Phys 14 (2012) 095015

5. Relic Axion searches in CAST: CAST-CAPP and RADES proposals

5.1. General Introduction to relic Axion searches

The nature of Dark Matter is one of the most important physics questions in these times. It is widely accepted that QCD Axions are an excellent candidate for the cold Dark Matter in our universe: Although the axion is very light, it can be non-thermally produced in the early universe. However, to this date only a few collaborations run experiments that are sensitive to QCD axions as Dark Matter. In consequence, only a very limited part of the Axion parameter space, in which it can be cold Dark Matter, has been searched. In addition, a huge parameter space of axion-like particles (Pseudoscalars predicted in Standard Model Extensions independently of the Strong CP problem) as Dark Matter remains to be explored.

Most axion Dark Matter searches, as also the ones proposed in this document, rely on the axion to two-photon coupling: If axions constitute Dark Matter, they should stream in large numbers through our experiments, being narrow band microwave resonators embedded in a strong magnetic field, here the magnetic field of the CAST magnet. In this magnetic field, axions would then be converted into photons and be visible at the resonant frequency of the cavity, related to the axion mass *m*. A high quality factor of the cavity pushes the probability of this process. Due to the pseudo-scalar nature of the axion, the external field and the cavity resulting electric field need to be parallel (see Figure 5.1 below).

In a very naive picture, the high-mass (i.e. high-frequency) parameter space for Dark Matter Axions is difficult to tackle in existing setups which run in solenoidal magnets. For high-mass axions, the cavity quality factor depletes (the cavity volume goes down), as the cavity's dimension *d* is lowered (figure below, left-hand side). In the dipole field of the long CAST dipole magnet, the volume can be kept large (long cavity), whilst the resonance frequency can be comparatively high, through the usage of relatively thin cavities. This implies, however, novel technical challenges as will be described later.

In the following, we present two proposals that aim to place a high-mass axion Dark Matter experiment in CAST. Having two setups with a different technical implementation and complementary mass range, makes us confident, through continuous exchange of experience, to overcome difficulties and find or exclude the axion in a well-motivated but so far uncharted parameter space of axion masses around ~20 micro-eV.

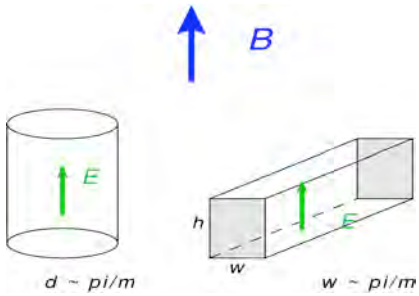

Figure 5.1 - Electric and magnetic fields in cavities for relic Axion searches (see text).

6. A Proposal to Search for Cold Dark Matter Axions with the Haloscope Technique Using the CAST Dipole Magnet

(The CAST-CAPP Detector) - (responsible L. Miceli)

[4]Joseph Brennan, [1]Hyoungsoon Choi, [2]MiRan Kim, [3]Yonuk Jung, [1]Jhinhwan Lee, [3]Yong-Ho Lee, [4]Frank Lincoln, [2]Lino Miceli, [1,2]Yannis Semertzidis, [1]Beom-Ki Yeo, [5]Eunil Won, [6]Walter Wuensch.

[1]Korea Advanced Institute of Science and Technology, Daejeon 305-701, Republic of Korea
[2]IBS Center for Axion and Precision Physics Research, Daejeon 305-701, Republic of Korea
[3]Korea Research Institute of Standard and Science, Daejeon 305-340, Republic of Korea
[4]Brookhaven National Laboratory, Upton, NY 11973, USA
[5]Korea University, Seoul, 136-713, Korea
[6]CERN, Geneva, Switzerland

6.1. Introduction and Motivation

Axions are one of the best motivated dark matter (DM) candidates. Arising as consequence of the Peccei-Quinn solution to the strong CP problem [1–7] they are a natural cold dark matter candidate [8–10] if their mass lies within the range of (1 – 100) μeV. This region is marked in orange in Figure 6.1. Beyond the explicit axion there is a wide range of so-called axion-like particles (ALPs) which have similar couplings but with an often increased coupling constant. They could also be good dark matter candidates [12,13]. Therefore, searches for axion and axion-like particle dark matter have great potential to shed light on one of the most important open questions in physics.

The possibility that axions or ALPs (from now on we will include axions whenever we say ALPs) are dark matter both allows and requires new search strategies. In contrast to searches for Weakly Interacting Massive Particles, scattering experiments are less suitable to search for ALP dark matter due to their extremely low masses. Hence one usually strives for inducing a conversion of ambient dark matter ALPs into detectable particles. Most of these searches are based on the coupling of ALPs to two photons,

$$\mathcal{L} \supset -g_{a\gamma\gamma}\phi_{ALP}F^{\mu\nu}\tilde{F}_{\mu\nu} = g_{a\gamma\gamma}\phi_{ALP}\mathbf{E}\cdot\mathbf{B}, \qquad (1)$$

where $g_{a\gamma\gamma}$ is the coupling constant with mass dimension −1 and ϕ_{ALP} denotes the ALP field. Searches employing microwave cavities, so-called haloscopes, have great potential for detecting ALP dark matter in the μeV mass range [14]. Indeed a number of searches using haloscopes have already been undertaken [15–17], such as the ADMX experiment [18,19]. The black “fingers” in Figure 6.1 show the corresponding experimental limits as a function of the ALP mass m_a.

Up to now all haloscope searches have used solenoid magnets to provide the magnetic field. Here we propose the use of rectangular cavities inserted in a dipole magnet, in a common experimental effort between the CAST collaboration and the Center for Axion and Precision Physics Research (CAPP), to which we will refer as the CAST-CAPP detector. This would be the first time in which the traditional haloscope technique is applied in rectangular, rather than cylindrical, geometry. Following the ideas in [23], this experiment would use the CERN Axion Solar Telescope (CAST) magnet [24] to search for ALPs in the ~ (2-3)x10^{-6} eV mass

range, with a sensitivity that could reach into the QCD axion domain. This region has never been explored before for cold DM searches. If approved, the experiment could start as early as the first half of calendar year 2016, much earlier than other planned experiments in the same mass range [25] as shown in Figure 6.2.

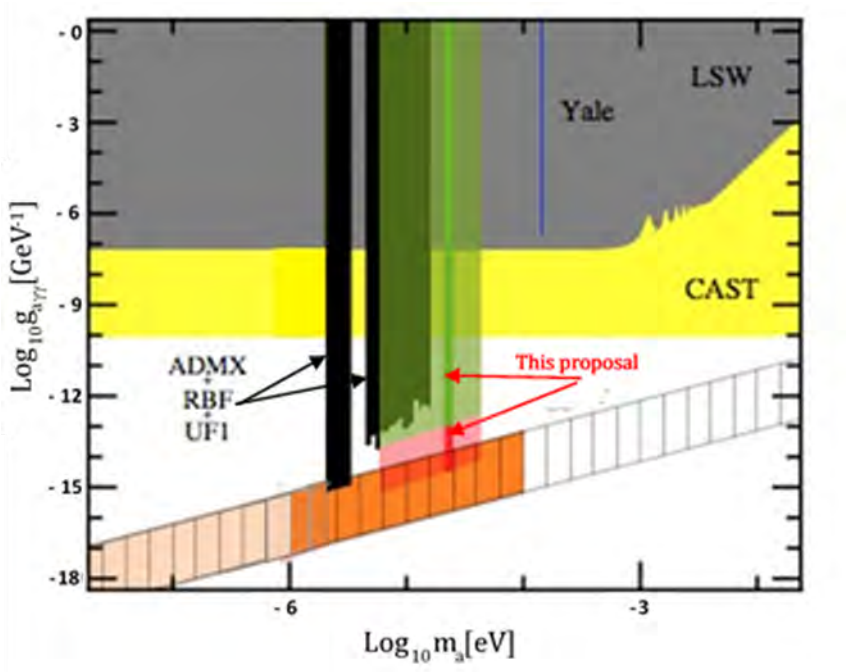

Figure 6.1 - Existing bounds for axion-like particles [15–21]. Compilation adapted from [41]. The QCD axion-region is marked as the hatched band. In the orange region axions are a natural candidate for dark matter. In the lighter shaded orange area axions can still be dark matter but with decreasing mass this requires an increasing amount of fine tuning [11]. Axion-like particles can be dark matter in a large part of the so far untested parameter space (cf. [12,13]). The light green (red) regions are the expected sensitivity of a dipole search for axion-like particle dark matter as described in [23]. The more solidly shaded part in the middle of this region corresponds to the region probed by a cavity with parameters as discussed in Sect. 3.

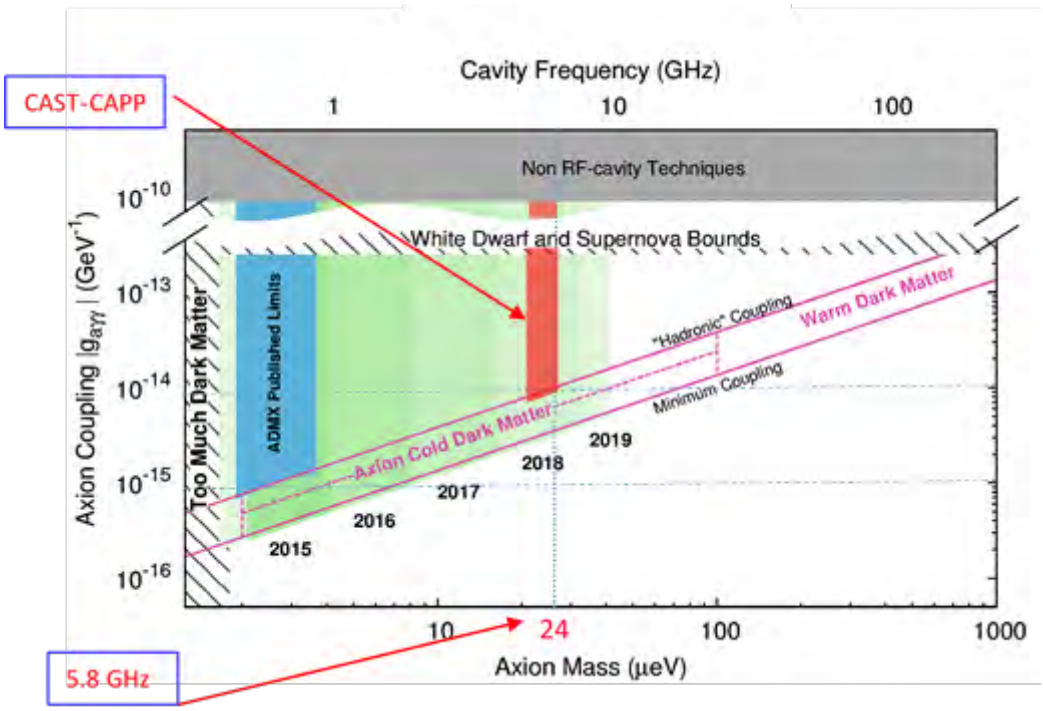

Figure 6.2 - The experiment proposed here (red-shaded regions) vs. the ADMX Gen-2 program [25] (green and blue regions).

6.2. Experimental Method

6.2.1.The Haloscope Technique

The principle of the haloscope is as follows. Dark matter axions entering a region permeated by a strong external magnetic field **B** will be converted into photons (corresponding to the electric field part in the interaction term (1.1)) which can then be detected. This conversion probability can be significantly enhanced if it occurs in a cavity resonant to the energy of the ALPs. Since ALPs are typically a cold dark matter candidate, their energy is given essentially by their mass. To cover a wide range of axion masses one therefore needs setups with cavities resonating at a range of different frequencies.

6.2.2. Rectangular Cavities in Dipole Magnets

Dipole magnets of proper geometry and sufficient field strength can enable the exploration of new ALP mass ranges. These type of magnets, available for instance at accelerator facilities, have not yet been exploited in searches for ALP DM. Such is the case of the CAST magnet, a 9.5T, ~ 9m-long superconducting dipole magnet, formerly a prototype of the LHC.

A suitable experimental setup in a dipole field for dark matter searches consists of tunable, rectangular cavities introduced into the magnet, with the magnetic field parallel to one of the resonator lateral sides. Equation (1) suggests that the sensitivity would be maximized if TE modes were used.

If we respectively indicate as w, h, and L the width, height, and length of the cavity, the transverse electric (TE_{mnp}) mode frequencies are given by

$$f_{lmn} = \frac{c}{2}\frac{1}{\sqrt{\epsilon\mu}}\sqrt{\left(\frac{l}{w}\right)^2 + \left(\frac{m}{h}\right)^2 + \left(\frac{n}{L}\right)^2} \tag{2}$$

In eq. (2) c is the speed of light, ε the permittivity, and μ the permeability of the cavity medium. The resonant electric field components inside the cavity, assuming its longitudinal side lines up with the z-coordinate, are

$$E_x = \frac{m\pi}{\varepsilon h} A_{lmn} \cos\left(\frac{l\pi}{w}x\right) \sin\left(\frac{m\pi}{h}y\right) \sin\left(\frac{n\pi}{L}z\right) \tag{3}$$

$$E_y = -\frac{l\pi}{\varepsilon w} A_{lmn} \sin\left(\frac{l\pi}{w}x\right) \cos\left(\frac{m\pi}{h}y\right) \sin\left(\frac{n\pi}{L}z\right) \tag{4}$$

$$E_z = 0 \tag{5}$$

In eq. (3) and (4) A_{lmn} are mode-dependent constants.
A suitable mode is TE_{101} if $w > h$ (TE_{011} if $h > w$). Indeed for the given cavity geometry this mode is the lowest possible mode, and the most favorable for the experiment. This is advantageous because the lowest resonant frequencies are usually the most isolated from other modes, whereas regions with overlapping modes can lead to reduction in sensitivity.
For TE_{l0n} modes the resonant field is

$$E_y \sim \sin\left(\frac{l\pi}{w}x\right) \sin\left(\frac{n\pi}{L}z\right) \tag{6}$$

Equation (6) can be used to calculate the geometry factor relevant for ALP DM searches [22],

$$C = \frac{1}{B_0^2 V}\frac{\left|\int \boldsymbol{B}\cdot\boldsymbol{E}dV\right|^2}{\int \boldsymbol{\varepsilon}(\boldsymbol{x})\boldsymbol{E}^2 dV} \tag{8}$$

where **E** is the electric field of the cavity, having volume V, and B_0 is the average, over the cavity volume, of the external magnetic field. Moreover, ε(x) is the dielectric permittivity inside the cavity. When using dielectric inserts, as discussed in Sect. 4 and 5, ε may depend on the position inside the cavity. For the cavity in question

$$C = \frac{0.66}{n^2} \qquad \text{for } n \text{ odd} \tag{9}$$

For all even *n* the geometry factor vanishes. In particular for $n = 1$ the geometry factor is 0.66.
While we refer to [23] for more general considerations about dipole searches, here we focus on what can be achieved with the standard operating parameters of the CAST magnet, summarized in Table 1.

Table 1. CAST magnet parameters[24]	
Physical Length	10 m
Magnetic Length	9.25 m
Actual operating B-field	9 T
Nominal bore size	43 mm
Number of bores	2
Operating temperature	1.8 °K

Assuming a bore size of 43 mm, the maximum outer lateral side of a cavity fitting inside this magnet would be 30 mm. For our estimates we will assume inner cavity lateral sizes of 25 mm X 24 mm. The fundamental frequency of such a cavity is 6.2 GHz that corresponds to an axion mass of 2.6 x 10^{-5} eV. In our scheme however, we plan to use a dielectric tuning mechanism, (Section 6.4), which lowers the maximum operating frequency in the fundamental mode to f_{101} = 5.8 GH corresponding to an axion mass of 2.4x10^{-5} eV.
This frequency (cf. the solid green/red area in Figure 6.1) is complementary to the ADMX setup [18-20] (black region in Figure 6.1) as well as to searches at Yale [21] (blue region in Figure 6.1).

6.3. Sensitivity

Following is an estimate of the sensitivity of the proposed experiment. The output power of a cavity with resonant frequency equal to the axion mass,

$$\omega = 2\pi f = m_a = 2\pi\times 0.24\ GHz \left(\frac{m_a}{10^{-6}eV}\right) \tag{10}$$

is given by Ref [22] (see also, e.g., Ref. [18]),

$$P = \left(g_{a\gamma\gamma}\right)^2 \rho_a \frac{1}{\boldsymbol{m_a}} B^2 C V\, min[Q_c, Q_a] \tag{11}$$

$$= 1.6\times 10^{-25}\mathrm{W}\times \left(g_{a\gamma\gamma}10^{15}\mathrm{GeV}\right)^2 \left(\frac{\rho_a}{300\ \mathrm{MeV/cm^3}}\right)\left(\frac{2.4\times 10^{-5}eV}{\boldsymbol{m_a}}\right) \times \left(\frac{B}{9\ \mathrm{T}}\right)^2 \left(\frac{\boldsymbol{C}}{0.66}\right)\left(\frac{V}{5\ l}\right)\left(\frac{Q}{5\times 10^3}\right)$$

where Q_c is the loaded[1] Q-factor and $Q_a \sim 10^6$ is the ALP dark matter Q-factor resulting from the energy-spread of the ALPs (see Eq. (13) below).
In the second part of the equation we have assumed $Q_c < Q_a$ as a further increase in Q does not increase the power. In the same equation, ρ_a, representing the dark-matter density in the vicinity of Earth, was set equal to a commonly used value of to obtain our estimate of the sensitivity. In the reminder of this section we address the necessary requirements to detect the resulting small power.
The time t needed to detect a given amount of power P with a signal to noise ratio SNR is determined by the Dicke radiometer equation [42],

$$SNR = \frac{P}{K_B T}\sqrt{\frac{t}{b}} \tag{12}$$

In the above equation T is the total system temperature, which is the sum of the physical temperature of the device plus the noise temperature of the receiver and amplifier chain, and b is the bandwidth in which the signal power is contained. In the ALP case the bandwidth of the signal is determined by the energy spread of the dark matter axions, which in turn is given by their velocity distribution. If we use the typical velocity spread of dark matter ALPs, expected to be $\Delta v_a \sim 300$ km/s $\sim 10^{-3}$c, the axion signal bandwidth is

$$2\pi b_a = \frac{m_a}{Q_a} = m_a\left(\frac{1}{\sqrt{1-\Delta v_a^2}} - 1\right) \sim 10^{-6} m_a \tag{13}$$

Therefore, deduced from (11) and (12), the time needed for a single measurement is,

$$t = (SNR)^2 \left(\frac{K_B T}{P}\right)^2 b_a \tag{14}$$
$$= 9 \times 10^9 s \left(g_{a\gamma\gamma} 10^{15}\text{GeV}\right)^{-4} \left(\frac{\rho_a}{300\ MeV/cm^3}\right)^{-2} \left(\frac{2.4\times10^{-5} eV}{m_a}\right)^{-3}$$
$$\times \left(\frac{SNR}{4}\right)^2 \left(\frac{T}{3.8\ ^\circ K}\right)^2 \left(\frac{B}{9\,\text{T}}\right)^{-4} \left(\frac{C}{0.66}\right)^{-2} \left(\frac{V}{5\,l}\right)^{-2} \left(\frac{Q}{5\times10^3}\right)^{-2} \left(\frac{10^6}{Q_a}\right)$$

If a coupling constant $g_{a\gamma\gamma} = 10^{-14}$ GeV^{-1} is assumed, we find that the time necessary to measure one frequency is ~ 10 days. In this estimate we have also assumed that we are able to fill the two CAST magnet bores with multiple cavities of total effective volume ~ 46%, a rather conservative Q = 5,000, and a system temperature of 3.8° K. The latter comes from adding the magnet operating temperature, 1.8 °K, with the noise temperature, ~2° K, of a commercially available low temperature High Electron Mobility Transistor (HEMT) amplifier. At $g_{a\gamma\gamma} = 10^{-13}$ GeV^{-1} this time would reduce to 1 min. At the frequency of our example, 5.8 GHz, we would then be able to reach deeply into yet unexplored regions of the axion search parameter space represented in Figure 6.1 (green finger) and Figure 6.2. Therefore with such a setup we definitely have an interesting sensitivity for ALP DM [13].
As the ALP mass is a priori unknown, an experiment should not only be sensitive to one mass but instead we would like to be able to scan a range of masses. Therefore it is important to determine the speed with which such a scan can be performed at the assumed signal-to-noise ratio. Since the bandwidth of the axion signal is smaller than the width of the cavity we can perform a simultaneous measurement of all potential ALP masses within the width of the cavity by doing a fast Fourier transform (FFT) of the output signal. Accordingly the scanning speed is determined by [18, 26],

$$\frac{df}{dt} = \frac{f}{Q}\frac{1}{t} \sim \frac{3.4\ KHz}{year}\left(g_{a\gamma\gamma} 10^{15}\text{GeV}\right)^4 \left(\frac{5.8\ \text{GHz}}{f}\right)^2 \left(\frac{4}{SNR}\right)^2 \left(\frac{3.8\ ^\circ\text{K}}{T}\right)^2$$
$$\times \left(\frac{B}{9\text{T}}\right)^4 \left(\frac{C}{0.66}\right)^2 \left(\frac{V}{5\,l}\right)^2 \left(\frac{Q}{5\times10^3}\right) \tag{15}$$

We see that with our benchmark cavity and the assumed values of the thermal noise and magnetic field strength, the scanning speed for couplings $g_{a\gamma\gamma} = 10^{-15}$ GeV^{-1} is in the order of a few KHz / year, whereas it is in a few tens of MHz/year range at $g_{a\gamma\gamma} = 10^{-14}$ GeV^{-1}, further demonstrating the good sensitivity to ALP DM of this setup.
The covered range could be extended by several GHz in the higher mass region for instance

---

[1] *"Loaded" in this context means that it is the Q-factor of the cavity coupled to the detector. Using an impedance matched cavity to optimize the power reaching the detector, one has Q = Q_0/2 where Q_0 is the unloaded Q-factor of the cavity alone.*

by constructing a series of 3 cavities each (down-) tunable by 20% and with frequencies up to ~10 GHz, while scaling the volume and quality factors appropriately. This corresponds to the lighter shaded area to the right of the green/red finger of Figure 6.1.

6.4. Cavity Design

6.4.1. Engineering Considerations

Since the experiment sensitivity increases with the resonator volume, it would be desirable to completely fill each of the two magnet bores with a single resonator or with phase-matched multiple cavities. As the aspect ratio L/w of the structure increases, however, the Q-value decreases and the resonant frequencies of the modes will converge to a single value, as seen in eq. (2) and, below, in eq. (16).
The unloaded Q-factor, Q_0, of the TE_{101} mode in a rectangular cavity as a function of its geometry, at room temperature, is given by,

$$Q_0 = \frac{c}{f_{101}\delta} \cdot \frac{h\left(w^2+L^2\right)^{3/2}}{2L^3(w+2h)+w^3(L+2h)}, \qquad \partial = \sqrt{\frac{1}{\pi f_{101}\sigma\mu}} \tag{16}$$

where δ is the skin-depth of the cavity walls, μ is the permeability and σ the conductivity of the metal [27]. At cryogenic temperatures (T ≤ 20□ K) and high frequencies (f ≥ 1 GHz), the mean free path of electrons in the copper becomes comparable with, or greater than, the classical skin depth given by Eq. (16). Then one enters the anomalous skin depth regime where $\delta \propto f^{-1/3}$ [28]. Hence significantly better values for δ can be achieved at lower temperatures[2].
If the aspect ratio L/w becomes large, Eq. (2) predicts that the modes converge towards a common resonant frequency. The frequency spacing, i.e. the distance in frequency to the next higher order mode, needs therefore to be considered.
If this spacing is small compared to the bandwidth of the cavity the two modes will couple to each other and exchange energy due to the resistive losses of the cavity, resulting in loss of sensitivity. Obviously it is desirable to operate in single mode, if not however, the loss in sensitivity at the desired frequency might still be acceptable.
For instance, if the minimum spacing between the resonant frequency of 2 modes, Eq. (17) is equal to their 6 dB bandwidth then only up to 25 % of the signal power might be lost through mode coupling.

$$\Delta f = f_{10n} - f_{10n-1} \approx f_{101} \cdot \frac{2n-1}{2} \cdot \left(\frac{w}{L}\right)^2 \tag{17}$$

This can be used as a criterion for the maximum cavity length [23]:

$$L_{max} = w\sqrt{\frac{(2n-1)\pi Q_0}{4}} = 2.6m\left(\frac{w}{2.5\ cm}\right)\left(\frac{2n-1}{3}\right)^{1/2}\left(\frac{Q_0}{5000}\right)^{1/2} \tag{18}$$

Eq. 18 is valid in the assumption that the Q factors of two neighboring modes are equal, for critical coupling and $f_{10n} \approx f_{101}$ in lowest order for small to moderate values of n.
Besides cavity length considerations, mechanical tolerances play a very important role in cavity manufacturing due to mode localization [26]. This means that the mode field

distribution in the resonator space is altered depending on the deviation of the cavity shape from its ideal design, thus causing a decrease in the geometry form factor (cf. Eq. 8) and, as a consequence, in the haloscope sensitivity to converted ALPs. To observe mode localization and investigate sensitivity to mechanical tolerances we have modeled a trapezoidal resonator in which the width of the cross section changes from w to w - Δw, and we have tracked the geometry form factor as a function of Δw, as reported in section 6.4.3.

6.4.2. Tuning Mechanism

A cavity can be tuned in several ways, the most straightforward being moving one of the sides (cf. Eq. 2). In our case this is not practical, nor desirable mainly due to difficulties in maintaining high conductivity under vacuum and at cryogenic temperatures. Instead we have studied tuning methods consisting in placing dielectric materials and/or metallic plates inside the cavity. Depending on its volume, position and shape, any material placed inside the cavity will change its mode structure and resonant frequency and, as a consequence, its quality and geometry factors. For a partially filled volume, pure TE and TM modes cannot propagate, whereas hybrid modes with weak field components in longitudinal direction are introduced.

Based on our models, we have concluded that the best compromise between having a sensible frequency tuning range, while maintaining good cavity sensitivity, is the use of dielectric material. While cavities with a relatively small L/w aspect ratio (up to ~ 10) can be readily tuned by introducing plates that are parallel to the small lateral sides and moving longitudinally, longer cavities are best tuned with dielectric bars that are placed parallel to the resonator long sides, as illustrated in Figure 6.3. These bars can be either made, for instance, of Sapphire or Alumina. A straightforward mechanical system makes them move towards the middle of the cavity. Electromagnetic waves inside the dielectric material propagate with a lower phase velocity, which changes the dispersion relations and the field in the cavity. The closer the dielectric bars to the center of the cavity, the lower its resonant frequency. The haloscope sensitivity is therefore shifted towards lower-mass ALPs. Model results of the tuning process are presented in Section 6.4.3.

6.4.3. A Cavity Solution for the CAST-CAPP Detector

We suggest a staged approach for the CAST-CAPP detector. In the first stage we would introduce two, phase matched, 50 cm-long cavities inside the magnet, one in each bore. A full-fledged experiment to exploit the entire magnetic length could be afforded at a later time, hinging on the success and experience of the first stage. Since the total volume of these two cavities is 12% of the value used in the example of Sect. 2, the sensitivity of this smaller haloscope would scale accordingly. The experiment would, however, still be able to easily reach into the unexplored region at $g_{a\gamma\gamma}\sim10^{-13}\mathrm{GeV}^{-1}$. A staged approach offers several advantages, such as the possibility of easier modeling, tuning, and thorough testing at cryogenic temperatures before insertion into the CAST magnet. The latter is important especially considering the magnet operational costs and its long warm-up cycle (~6 weeks).

With this approach in mind, we have started modeling a 2.5 cm x 2.4 cm x 50 cm tunable rectangular cavity using COMSOL Multiphysics [29]. This cavity geometry is well within the limits of reliable TE_{101} (or TE_{011}) mode of operation as indicated by Eq. 18.

---

2 *The DC conductivity of metal is increased at cryogenic temperatures by the residual resistance ratio (RRR), values of ≈ 200 are realistic for pure copper [27]. Nonetheless strong magnetic fields can influence charge carriers in the metal (magnetoresistance), therefore reducing its conductivity by a factor of ≈ 15 [28].*

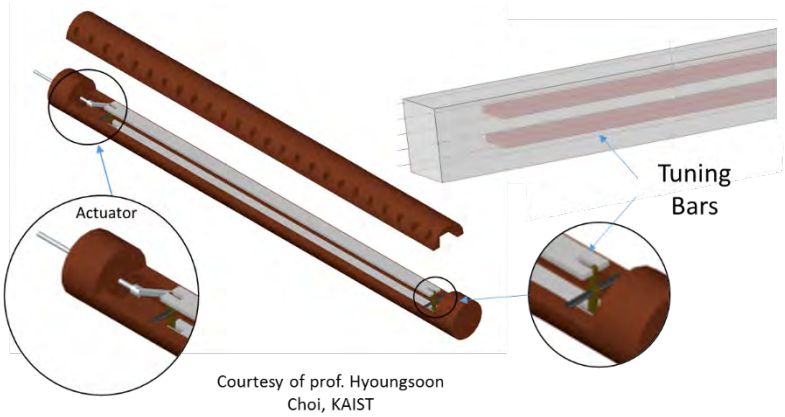

Figure 6.3 - Conceptual engineering design of a possible tuning solution for a 2.5cm x 2.4cm x 50cm prototype cavity with dielectric tuning bars. The cavity is tuned by one single piezo actuator placed externally, while the bars are kept parallel to each other. This image does not necessarily represent the way in which the cavity will be assembled.

Resonant frequencies in this simulation are reproducible to 5 parts in 10,000, quality and geometry factors to 1%. The model accuracy can be increased as needed at the cost of software running time.
As suggested by the conceptual design represented in Figure 6.3, the resonator can be tuned by a single, externally placed piezo actuator. The bars move parallel to each other towards, or away from, the center while slightly shifting in opposite directions along the cavity axis.
In this model, whose quantitative results are in part represented in the Figures 6.4 and 6.5, the tuning bar sizes are 2.5 mm x 15 mm x 45 cm, providing a tuning range of more than 20%, from 5.8 to 4.6 GHz, with a penetration distance from the cavity walls of up to 8 mm. The quality and geometry factors change significantly while tuning. Their product, however, and the experiment sensitivity with it, stays nearly constant, as shown in the right hand side plot of Figure 6.5.

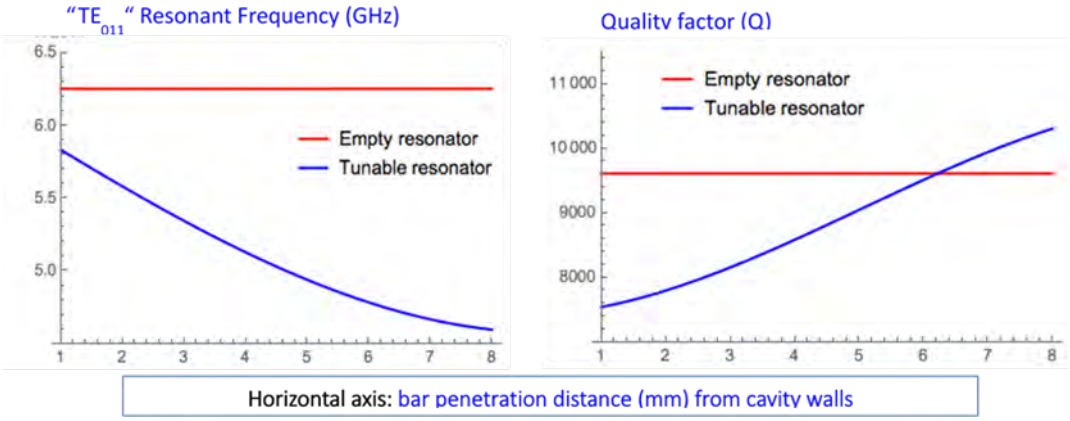

Figure 6.4 - Modeling of a 2.5cm x 2.4cm x 50cm cavity with dielectric tuning bar size 2.5mm x 10mm x 45 mm. Resonant frequency and quality factor (Q) of fundamental mode as a function of bar penetration distance.

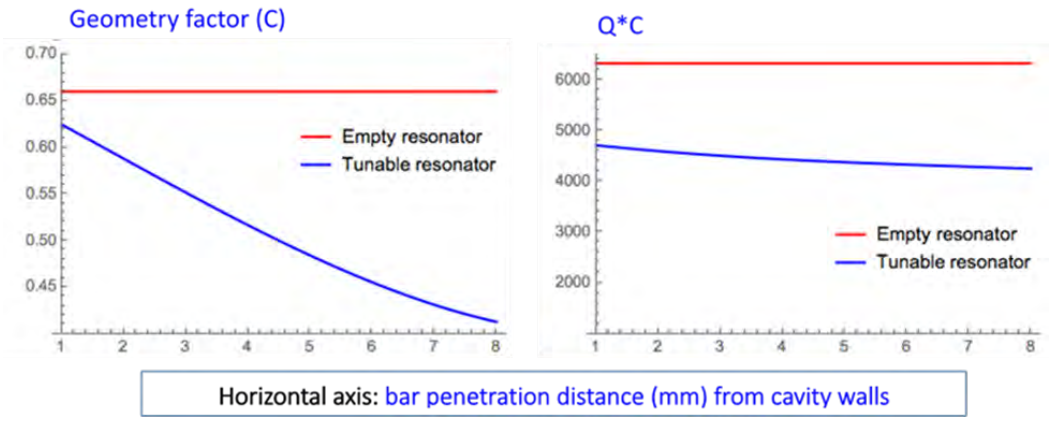

Figure 6.5 - Modeling of a 2.5cm x 2.4cm x 50cm cavity with dielectric tuning bar size 2.5mm x 10mm x 45 mm. Geometry factor (C) and the product Q*C, of fundamental mode as a function of bar penetration distance.

Figure 6.6 shows the electric field profile and distribution inside the resonator at bar penetration distance equal to 1 mm. The inset in the same figure provides a visual of the statement at the end of section 6.4.2.

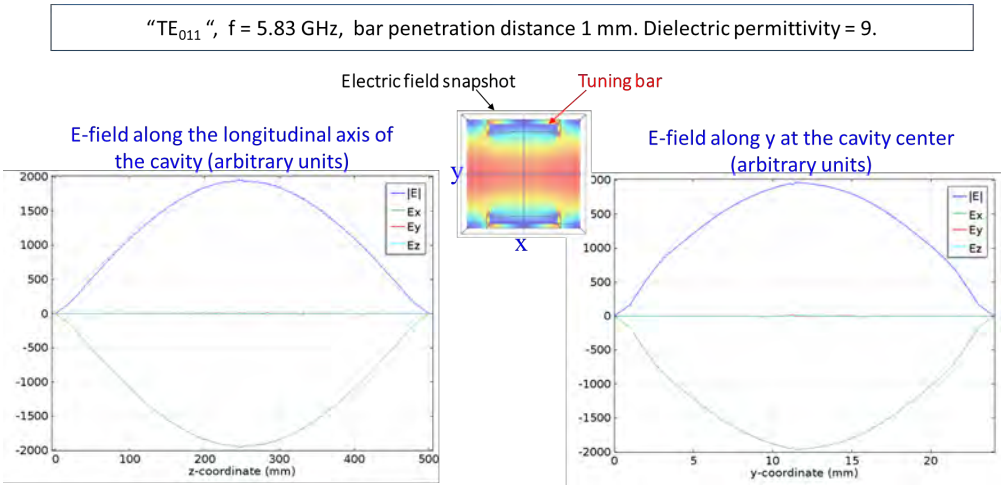

Figure 6.6 - The electric field inside the resonator when the dielectric tuning bars are at a distance of 1 mm from the cavity walls. Notice how the electric field distribution is altered by the presence of the tuning bars. The field is more intense in the red, compared to the yellow, areas of the XY map (inset).

Mechanical tolerances are another crucial aspect of cavity engineering, becoming more demanding with increasing longitudinal-to-transverse aspect ratio. As pointed out in Section 6.4.1, mechanical non-uniformities or deformations give rise to mode localization, thus decreasing the geometry factor. This is illustrated in Figure 6.7, representing a deformation of the same resonator, without tuning bars. The width of the resonator was changed on one side from 24 mm to 23.5 mm, while maintaining the opposite side constant, thus giving the resonator structure a trapezoidal shape. In the same figure, the geometry factor variations and the two snapshots of the electric field clearly illustrate mode localization. For a 50 cm long cavity this is not an issue, since readily achievable mechanical machining and assembly accuracy in the order of 50 μm are sufficient to maintain constant sensitivity, as inferred from the same figure.

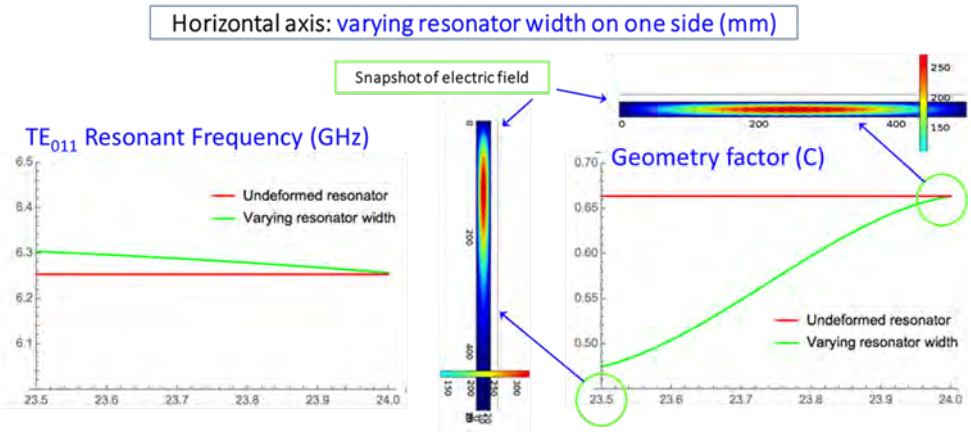

Figure 6.7 - Mechanical tolerances and mode localization in a 2.5cm x 2.4cm x 50cm cavity.

6.5. Tentative Timeline and Conclusions

In the assumption that only one magnet bore will be available for this experiment, a sensible approach could be the following:

Year 2016: One, 50 cm long cavity, of lateral sizes as in Section 6.4, is proposed. In this approach, the Piezo-actuators for the tuning mechanism and for the cavity coupling ports, and the cryo (HEMT) amplifier can be placed outside the magnet bore in a region of low B-field compared to the magnet operating field, thus simplifying the experiment. This apparatus should be able to reach a sensitivity of $g_{a\gamma\gamma}=10^{-13}GeV^{-1}$, requiring ~ 7 days to measure a single frequency. In this estimate a more conservative loaded Q of 1,000 has been assumed, compared to Section 6.4.

During this time, in view of future multiple cavity operation, we propose to introduce an additional small cavity, placed deeper inside the magnet, to study the HEMT amplifier response and the behavior of the tuning mechanism in high magnetic field, and to attempt phase matching the two cavities.

Year 2017: Hinging on the experience of the previous year, we propose to run an experiment inclusive of an additional two, phase matched, ~ 100 cm long cavities. According to equation (18) we should still be able to operate these resonators in the fundamental TE mode.

Year 2018: Fill the entire magnet bore with multiple phase-matched cavities.

The following concluding remark is in order. The CAPP is developing a systematic approach to cold dark matter axion search supported by a significant R&D, inclusive of studies of phase matched multiple cavities and low noise, near quantum-limited amplifier research, and superconductivity in the presence of high magnetic fields.

These already started efforts, will be beneficial to the CAST-CAPP/IBS experiment, if approved, particularly if we consider that several players of the CAPP R&D have pledged to support and contribute to the CAST-CAPP experiment.

References

[1] R. D. Peccei and H. R. Quinn, Phys. Rev. Lett. 38, 1440 (1977).
[2] S. Weinberg, Phys. Rev. Lett. 40, 223 (1978).
[3] F. Wilczek, Phys. Rev. Lett. 40, 279 (1978).
[4] J. E. Kim, Phys. Rev. Lett. 43, 103 (1979).
[5] M. Dine, W. Fischler, and M. Srednicki, Phys. Lett. B104, 199 (1981).
[6] M. A. Shifman, A. I. Vainshtein, and V. I. Zakharov, Nucl. Phys. B166, 493 (1980).
[7] A. R. Zhitnitsky, Sov. J. Nucl. Phys. 31, 260 (1980).
[8] J. Preskill, M. B. Wise, and F. Wilczek, Phys. Lett. B120, 127 (1983).
[9] L. F. Abbott and P. Sikivie, Phys. Lett. B120, 133 (1983).
[10] M. Dine and W. Fischler, Phys. Lett. B120, 137 (1983).
[11] M. P. Hertzberg, M. Tegmark, and F. Wilczek, Phys.Rev. D78, 083507 (2008).
[12] A. Arvanitaki, S. Dimopoulos, S. Dubovsky, N. Kaloper, and J. March-Russell, Phys. Rev. D81, 123530 (2010).
[13] P. Arias, D. Cadamuro, M. Goodsell, J. Jaeckel, J. Redondo, and A. Ringwald, Report No. DESY 11-226; Report No. MPP-2011-140; Report No. CERN-PH-TH/ 2011-323; Report No. IPPP/11/80.
[14] P. Sikivie, Phys. Rev. Lett. 51, 1415 (1983).
[15] S. De Panfilis et al., Phys. Rev. Lett. 59, 839 (1987).
[16] W. Wuensch et al., Phys. Rev. D40, 3153 (1989).
[17] C. Hagmann, P. Sikivie, N. S. Sullivan, and D. B. Tanner, Phys. Rev. D42, 1297 (1990).
[18] S. J. Asztalos et al., Phys. Rev. D64, 092003 (2001).
[19] S. J. Asztalos et al. (ADMX Collaboration), Phys. Rev. Lett. 104, 041301 (2010).
[20] S. J. Asztalos et al. (ADMX Collaboration), Phys. Rev. D69, 011101 (2004).
[21] A. Martin, The 6th Axion-WIMP-WISP Workshop on Mykonos, Hamburg, Germany, 2011 (unpublished), http://axion-wimp.desy.de.
[22] P. Sikivie, Phys. Rev. D32, 2988 (1985), **36**, 974(E) (1987).
[23] O. Baker et al., Phys. Rev. D85, 035018 (2012).
[24] K. Zioutas *et al*. (CAST Collaboration), *Phys. Rev. Lett*. 94 (2005) 121301.
[25] T.M. Shokair et al., arXiv:1405.3685, A. Rybka, IBS-MultiDark Joint Focus Program: WIMPs and Axions, 10-21 October 2014, IBS Center for Theoretical Physics of the Universe (CTPU), Daejeon, Korea, https://indico.ibs.re.kr/event/7/.
[26] R. G. Chambers, Proceedings of the Royal Society of London. Series A, Mathematical and Physical Sciences 215, pp. 481 (1952).
[27] M. Koratzinos, Chamonix 2011 Workshop on LHC Performance, 149 (2011).
[28] J. E. Huffman, M. L. Snodgrass, and F. J. Blatt, Phys. Rev. B 23, 483 (1981).
[29] COMSOL Multiphysics version 5.0 on MS Windows 7 Professional Operating System.

7. Relic Axion Detector Exploratory Setup: RADES in CAST

I. Irastorza, J. Redondo (Zaragoza U.), B. Gimeno, M. Guglielmi, C. Cogollos, V. Boria (Valencia. U), B. Doebrich (CERN)

7.1. Introduction

Axions are prime candidates for the dark matter of the universe. They are motivated extremely good in theories beyond the standard model like string theory and from the phenomenological point of view by being a direct consequence of the Peccei-Quinn solution of the strong CP problem, probably the simplest and most elegant found so far. The theoretical, phenomenological and experimental communities are experiencing a very strong rise of interest in axions in recent years.
The existence of axion dark matter to some extent is completely unavoidable in the parameter space that has not been excluded by laboratory experiments, helioscopes like CAST and astrophysics. Axions are excellent cold dark matter candidates in essentially all the mass range in which they are not excluded

$$m_a < 10meV. \tag{1}$$

However, the simplest cosmological scenarios favor certain benchmark ranges to bear in mind (explained later on),

$$m_a \in 115 \pm 25\mu eV, (postinflationPQ) \tag{2}$$
$$m_a \in (1,500)\mu eV, (preinflationPQ + naturalness). \tag{3}$$

The most promising experimental technique to search for axion dark matter in this mass ranges is Sikivie's haloscope –a high-Q microwave cavity immersed in a strong B-field parallel to the electric field of a resonant mode. The axion dark matter field excites the resonant mode when the axion mass coincides with the resonance frequency $\nu_0 = m_a/2\pi$,

$$\nu = 0.2424\frac{m_a}{\mu eV}GHz. \tag{4}$$

The excited power is to be extracted with an antenna, amplified with a low-noise amplifier and recorded. The signal is so weak that it is swamped by thermal and electronic noise from the first amp and has to be integrated over relatively long times.
The main difficulty of these experiments is that we don't know the axion mass, so the signal is to be searched by tuning the cavity to sweep a relatively large band with adequate resonance modes. The signal bandwidth is determined by the energy dispersion of dark matter axions in the galaxy $\Delta\nu_0 \simeq 10^{-6}\nu_0$. The broader interesting region mentioned is 0.24 - 120 GHz, which contains $\sim O(6\times10^6)$ channels where the axion signal could be. No experimental apparatus conceived can cover this number with the sensitivity required in a reasonable amount of time, one needs a wealth of different cavities.
There are several ongoing experiments and proposals in particular bands of the frequency range: ADMX (2 - 4μeV), ADMX-HF (16 - 24μeV), CARRACK ($m_a \sim 10\mu$eV range, but apparently on standby), YMCE ($m_a \sim 141\mu$eV), ... and a recently created IBS institute (CAPP) created to push the sensitivities of the different parameters involved to the maximum

and ensure the ultimate generation of axion dark matter experiments. CAPP is involved in a proposal to search axion DM in CAST, presented in this same document.
With the humongous number of channels to be explored there is ample room for different collaborations to jump in and explore a particular frequency band. Higher frequencies are particularly cumbersome because the signals are typically weaker, the cavity technology more sensitive to precision manufacturing and the noise levels are higher. Here a key parameter can be the volume of the cavity, which drives linearly the signal power expected from axions. The experimental proposals devised so far exploit the highest quality cavities, which tend to be cylindrical cavities with diameters comparable with half wavelength of the desired frequency. Higher frequency devices like YMCE are thus very small and expect tiny signals. They need to rely on boosting other parameters to compensate.
An interesting direction was implied in a recent publication [1]. The intense B-fields of dipole accelerator magnets such as the one employed by CAST can be used to search for axion DM with long rectangular cavities[1]. It turns out that the fundamental mode of a long rectangular cavity ($\nu = \sqrt{w^{-2} + L^{-2}}$ /2 with height, width, length $= h < w < L$) is not much affected by L, nor is the quality factor. However, the volume of the cavity increases linearly with L and so does the signal power due to axions. The drawbacks of large volume cavities are : 1) resonant modes are closer together than in a more proportionate cavity and the tuning range without mode crossings is narrower, 2) mode localization can be an important issue if mechanical tolerances are not controlled, 3) large volume magnets to host the cavities can be costly.
Many of these drawbacks have an interesting resolution if the International Axion Observatory (IAXO) is approved and its huge magnetic toroid is made suitable for dark matter searches. The total volume available is O(15000) liters with an average B-field of 2.5 T, to be compared for instance with the ADMX cylindrical cavity of 140 liters at 8 T. The volume is so huge that one can instrument it with a plethora of large volume cavities optimized at different frequencies each having a much smaller running range. If still the signal is not strong enough cavity outputs can be also combined in parallel. The issue of mechanical tolerances it is still however a problem. With this future in mind, it seems reasonable to start developing designs where testing the main issues that we will find in future large-scale axion DM searches.
We think that the B-field of the CAST dipole magnet is very well suited to host different axion DM pilot experiments. The goal would be to explore un-scanned axion masses and use the experiments to investigate tuning mechanisms, the impact of tolerances at high frequencies and so pave the road towards a full scan of the axion DM parameter space.
We have started a collaboration to build, characterize and instrument those cavities with theoretical support to optimize the axion production and detection. The groups participating are U. Zaragoza, U. Valencia, CERN.
We thus raise the proposal to the CAST collaboration to participate in the experiment by allowing the use of one of the CAST magnet bores to host our DM experiments, as well as helping with running of the magnet, operation of cryogenics, etc.

7.2. **Experiment**

Our proposed experiment consists on a resonant cavity in the form of a tunable Chevyschev-like filter. The cavity is to be placed in the cold bore of CAST, with the output antenna placed in the outmost cavity module. The signal is extracted from the cavity through a coaxial cable and amplified by a low-noise HEMT amplifier, still connected to the cold mass and possible inside a magnetic shielding to decrease the effect on the amp performance. The resulting signal is mixed down in frequency and recorded in a PC.

The axion dark matter field at Earth ($\theta(t) \sim \theta_e \cos(m_a t) \sim 2.6 \times 10^{-19} \cos(m_a t)$ for the canonical local DM density $\varrho_{DM} = 0.3$ GeV/cm^3) excites resonant cavity modes through the axion coupling to two photons

$$\mathcal{L} = c_\gamma \frac{\alpha}{2\pi} \theta B \cdot E \tag{5}$$

allowing to extract a power from the in-tune cavity given by

$$P_a = \kappa g_{a\gamma}^2 \frac{1}{m_a} B^2 \rho_{DM} V Q \mathcal{G} = \kappa \left(\frac{c_\gamma \alpha}{2\pi}\right)^2 \theta_e^2 m_a B^2 V Q \mathcal{G} \tag{6}$$

$$= 6.5 \times 10^{-24} Watt \frac{\kappa}{0.5} \left(\frac{c_\gamma}{1.9}\right)^2 \frac{m_a}{20\mu eV} \left(\frac{B}{9T}\right)^2 \frac{V}{1l} \frac{Q}{10^4} \mathcal{G} \tag{7}$$

in a bandwidth $\Delta\nu \simeq 10^{-6} m_a/(2\pi)$ where B is the B-field average intensity, V the cavity volume, $\varkappa$ the cavity coupling efficiency, and $\mathcal{G}$ is a normalised overlap function between the cavity mode and the B-field

$$\mathcal{G} = \frac{\left(\int dV\, E_{mode} \cdot B\right)^2}{B^2 V \int dV |E_{mode}|^2}, \tag{8}$$

which is typically of O(1) for cleverly selected modes.
This tiny signal is usually swamped by thermal and amplifier noise

$$P_T = \left(\frac{\omega}{e^{\omega/T} - 1} + \omega + T_{amp}\right) \Delta\nu \xrightarrow{\omega = m_a \ll T} 3.3 \times 10^{-19}\, \text{Watt} \frac{T + T_{amp}}{5\text{K}} \frac{m_a}{20\,\mu\text{eV}}, \tag{9}$$

where we have assumed noise above the quantum limit $\omega \ll T$.
A resonant mode with a Q-factor Q has a line width which contains a number of axion mass channels

$$\# \sim \frac{10^6}{Q} \tag{10}$$

so that with the cavity tuned to a given frequency one can measure simultaneously all these channels (readout electronics and storage permitting). The tuning steps are then of order ν/Q. Using Dycke's radiometer equation, $S/N = P_a \sqrt{\Delta\nu t}/P_T$, the sensitivity for the axion-photon coupling c_γ demanding a given signal to noise ratio S/N after a measurement time t tuned at the same central frequency is

$$c_\gamma|_{reach} \simeq 13 \left(\frac{S}{N}\right)^{\frac{1}{2}} \frac{9T}{B} \left(\frac{1l}{V}\right)^{\frac{1}{2}} \left(\frac{10^4}{Q}\right)^{\frac{1}{2}} \frac{1}{\sqrt{\mathcal{G}}} \left(\frac{10K}{T_{eff}}\right)^{\frac{1}{2}} \left(\frac{0.5}{\kappa}\right)^{\frac{1}{2}} \left(\frac{20\mu eV}{m_a} \frac{hour}{t}\right)^{\frac{1}{4}}.$$

With a relatively large volume cavity (10l), a large measurement time ($\sim$ *day*) and these out-of-the-box noise figures (standard HEMT amplifier+thermal noise), KSVZ axions ($c_\gamma = 1.9$) can be tested at these large masses. Of course, for a very narrow axion mass range of order $\sim m_a/Q$, O(0.02 μeV) in this case for instance. With a more sophisticated first amplifier one can reasonably improve the sensitivity a factor of $\sim\sqrt{2}$ and with a quantum limited SQUID or JPA ($20\mu eV = 232$ mK) bury it under the thermal noise expected inside the CAST magnet. At the moment it is hard to conceive how to implement a 250 mK cryostat inside the CAST bore

to host a sizable volume cavity, so we must stick as $\sim$ 1.9 K as our irreducible noise figure. Commercial HEMT amplifiers with noise temperature $\sim$ 3 K seem to be available in the 6 GHz frequency range.
To cover a larger mass range, one repeats measurements after retuning the cavity. Assuming that the time taken to tune the cavity and any necessary calibration is smaller than the measurement time, which is typically the case for our setups, the scanning rate: axion mass (frequency) band per unit time is given by

$$\frac{dm_a}{dt} = 2\pi\frac{d\nu}{dt} \sim \frac{m_a/Q}{(S/N)^2(P_T/P_a)^2/\Delta\nu} \quad (11)$$

$$\sim 0.7\frac{neV}{day}\left(\frac{S}{N}\right)^{-2}\left(\frac{B}{9T}\right)^4\left(\frac{c_\gamma}{1.9}\right)^4\left(\frac{m_a}{20\mu eV}\right)^2\frac{Q}{10^4}\left(\frac{V}{10l}\right)^2\left(\frac{T}{10K}\right)^{-2}\mathcal{G}^2. \quad (12)$$

With this figures, a $\sim$ $O(year)$ measurement campaign can cover a $O(10\%)$ band around the central axion mass with sensitivity to KSVZ axions working a bit on the noise figure. This is a final goal that we plan to achieve after building, instrumenting and measuring with intermediate setups we describe in the following.

Base test (2016)
In a first version of the apparatus the tuning mechanism will not be available, and the mass range to be scanned will be fixed from the beginning. We are designing a cavity shaped like a 5-pole filter of external dimensions (width, height, length ~ 35,25,200 mm) with a strong resonant mode at $\sim$ 6 GHz an unloaded Q-factor of $\sim$ 10^4, see Figure 7.1. These Chebyschev-like structures are resonant cavities coupled by relatively large irises where only evanescent modes exist. When the fundamental mode of the uncoupled cavities is alike, the coupling breaks the degeneracy producing a controllable pass-band filter around frequencies related to the fundamental of one cavity. In a n-pole filter there are n-resonant modes whose positions can be optimized to enlarge the band of the filter or to obtain desirable properties. The design of these filters is nowadays very automatized. We are using FEST3D to design and optimize the different parameters (cavity dimensions, breadth of the irises, etc.)

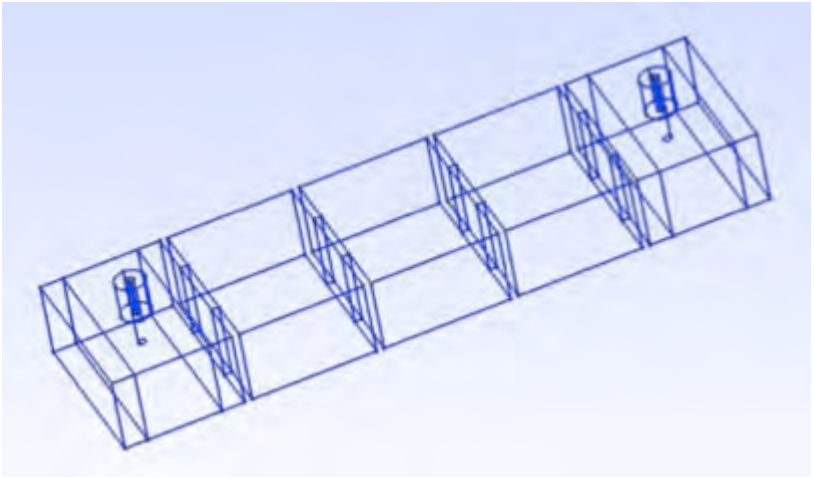

Figure 7.1 - Sketch of the base filter-like cavity proposed for the first test with coaxial inputs in the first (measurement output) and last (test input).

In this simple picture of the resonance frequencies track closely those of the fundamental mode of one of its cavities (short-circuited), i.e. very roughly

$$\nu \sim \frac{1}{2}\sqrt{\frac{1}{w^2}+\frac{1}{L^2}} \sim 6GHz\frac{35mm}{w}\sqrt{\frac{1+(wL)^2}{2}} \tag{13}$$

where w and L are the width and length of one of the single cavities. Thinking about maximizing the Volume of our experiment inside CAST we find figures of w,L ~35 mm. Increasing the number of poles one can get a higher quality filter with a broader band, but the sensitivity to manufacturing tolerances is larger and we have to assess how far we can go.

This geometry is to be compared with a simpler rectangular cavity of width of dimensions w,h,L, whose fundamental mode is also given by equation (13) but where now L is typically much longer than w (if is to be optimized for CAST) and thus $\nu \sim 1/2w$. Interestingly, the filter-like cavity can have a larger width for the same fundamental mode frequency, which allows to increase the volume and thus the axion signal. From a complementary perspective, for a fixed volume (such as the case for CAST), these cavities can search for axions at higher frequencies.

We plan to have the cavity by the end of 2015 and a first acquisition system with cryogenic and strong B-field requirements by spring 2016. During the rest of 2016, we plan for a experimental program including installation of the cavity in the CAST bore, commissioning, test runs and, if successful, a physics run, all lasting a few months.

The sensitivity of this setup will be limited, with the numbers mentioned above we show it in Figure 7.2 for a live-time of one month, which reaches $c_\gamma \sim 10$ in a narrow band (Black region) and therefore nor sufficient to popular QCD axion models like KSVZ. However, it will be sufficient to probe DM parameter space so far unexplored.

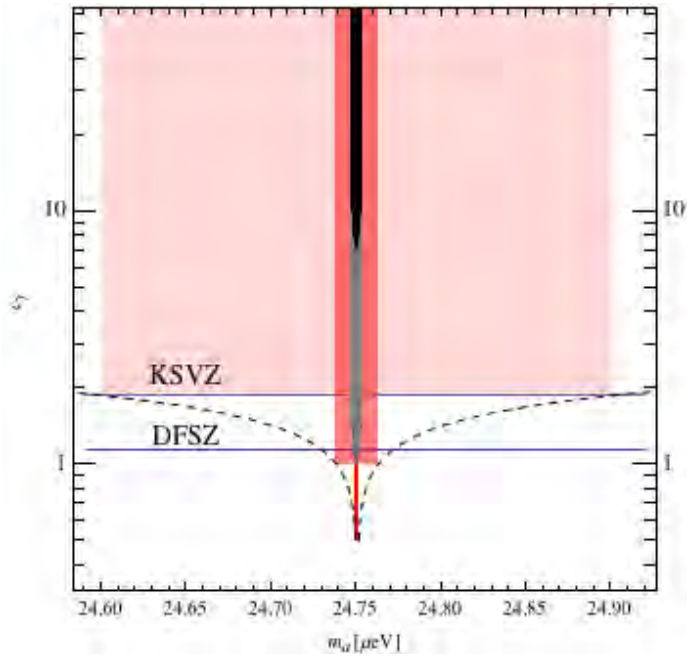

Figure 7.2 - Sensitivity of CAST axion DM experiments outlined in this proposal. Base test with 5 poles and 200 mm length (black region), an ideal maximum with a large number of poles filling the magnet (gray region). Each assumes a live-time of a month with T = 5 K noise levels. A one year data taking campaign with the tunable version can cover a mass band with sensitivity given by the dashed line. Examples are the red narrow band which reaches c_γ = 0.5 in a 0.4 neV band, the fainter red band reaching c_γ = 1 in a 6 neV band or the much broader light-red region exploring KSVZ couplings within .1 μeV.

Towards longer cavities (2017)

In parallel with the preparations for the base cavity and acquisition system we shall begin a systematic program of designing and building filter-like cavities of increasing number of poles. Prototypes with O(m) length shall be prepared and the maximum length investigated. The maximum allowed by CAST is $O(9m)$. By 2017 we might be in position of taking a few months of data with one or several of these longer cavities. The maximum reach with reasonable parameters (T = 5 K, width, height~ 35,25 mm, 1 month live-time) and without any tuning is shown in Figure 7.2 as a gray band. It has the potential to reach KSVZ axions (c_γ = 1.9) in a narrow band.

Tuning and mode crossing

The final goal is to be able to design a tunable cavity where we can extend the axion search to a sizable band with reasonable sensitivity. Preliminary calculations show however that it is extremely difficult to survey below KSVZ sensitivity (c_γ = 1.9) in a band much larger than a few percent. It seems wise to confine our experiment to a narrow band where results are highly relevant than to a much broader band without sufficient sensitivity. In this case, the tuning mechanism can be also considerably simplified. In order to commission such an experiment we need to work on three front-lines, decrease the receiver's noise, enlarge the volume and design a mechanism to tune the cavity.

Tuning to some extent can be envisaged by adding small dielectric insets or copper screws to each of the cavity modules. In the first set ups, these can be operated manually but this is not a possibility for a broadband data taking campaign because the experiment cannot be warmed up every time one needs to re-tune the cavity. Thus, the cavities have to be endowed with a mechanical link with the outside or a remotely operated motor to control the screws. We will optimize the number of tuning units needed to have as little as possible given our frequency range of interest.

The noise level can be conceivably decreased by using a SQUID or JPA, at the price of complicating slightly the implementation since these devices require low B-fields to work properly and magnetic isolation would need to be improved. However, without lower temperatures the gain is relatively modest compared with low noise HEMT.

References

[1] O. K. Baker, M. Betz, F. Caspers, J. Jaeckel, A. Lindner, A. Ringwald, Y. Semertzidis, P. Sikivie, K. Zioutas, Phys. Rev. D **85** (2012) 035018 [arXiv:1110.2180 [physics.ins-det]].

8. **Projected CAST proposal time schedule** – (*G. Cantatore, K. Zioutas)*

	2016	**2017**	**2018**
InGRID	• upgraded search for solar chameleons with: o improved mesh signal readout o active cosmic muon veto o ultra-thin window		
KWISP	• solar tracking with room temperature membrane • study homodyne detection	• solar tracking with homodyne detection • study membrane cooling	• solar tracking with cooled membrane and homodyne detection
The CAST-CAPP Detector	• initial search with one 0.5 m long cavity • Study of HEMT amplifier response in high magnetic field	• Search with two phase-matched ~ 50 to 100 cm-long cavities inside a single magnet-bore • Study of tuning mechanisms for higher order modes	• Filling one magnet bore with multiple cavities, conditioned to funds availability.
RADES	• base test with fixed 200 mm cavity	• tests with O(m) long cavities	

9. **Summary** – (Responsible K. Zioutas)

CAST has gained so far a world wide "good" reputation with its search for solar axions and chameleons with state-of-the-art equipment and novel ideas. Even though in the already performed investigations no signal for new physics has been found, CAST provided world best limits. The initially estimated CAST performance for solar axions has been surpassed, while its field of research has been extended with the pioneering solar chameleon measurement end of 2013. The previous sections show that CAST has new potential to justify its operation as an astroparticle physics telescope, entering deeper into the fascinating sector of dark energy (chameleons) and dark matter (relic axions). The collaboration with external people remains instrumental for keeping CAST physics reach in the forefront, while all detector systems used (or to be used) are home made.

We like to point-out that the recently introduced detection concept [1)] for solar chameleons with a supersensitive force sensor reached already in the lab (INFN/Trieste) the nominal value and is there in operation. It seems that a considerable improvement of its performance, even at room temperature, is possible. Therefore, the ongoing investigations in Trieste along with the R&D work in progress there are essential for the chameleon search. However, once a force sensor is commissioned and takes data in CAST, hopefully soon in 2015, its solar chameleon sensitivity should increase by a factor of ~100, or even much more, thanks to the large effective area of the XRT (from MPE). And this, with a unique particle ID scheme as the Sun is moving across the f.o.v. even of the XRT being stationary at the very beginning.

In short, the proposed new CAST physics reach has a discovery potential in the forefront of astroparticle physics, and this at lowest cost, utilizing, as in the past, resources and know-how from CERN and home Institutes. We refer throughout this proposal to relic axions and chameleons as generic particles CAST can be sensitive to. Interestingly, after more than 15 years, CAST is still motivating and attracting people.

[1)] One of us (K.Z.) wish to recall that the very first encouraging feasibility study of a sensitive force sensor was worked out with Keith Baker and Jack Harris during his visits to Yale University from 2011 onwards. The obtained results were used in previous CAST annual reports to the SPSC.